A REPORT FROM

OWENS-ILLINOIS TECHNICAL CENTER

FORM NO. 605 K

SEMI-ANNUAL TECHNICAL REPORT
BY: ROBERT W. BECK

DAMAGE THRESHOLD STUDIES OF GLASS LASER MATERIALS

31 JANUARY 1970
CONTRACT NO DAHC15-69-C-0303

CONSUMER & TECHNICAL PRODUCTS DIVISION
RESEARCH, DEVELOPMENT & ENGINEERING

OWENS-ILLINOIS
GENERAL OFFICES TOLEDO 1, OHIO

SPONSORED BY:
ADVANCED RESEARCH PROJECTS AGENCY
ARPA ORDER NO 1441
PROGRAM CODE P9D10

SEMI-ANNUAL TECHNICAL REPORT
BY: ROBERT W. BECK

DAMAGE THRESHOLD STUDIES OF GLASS LASER MATERIALS

31 JANUARY 1970
CONTRACT NO DAHC15-69-C-0303

CONTRACT DATE	30 JUNE 1969
CONTRACT EXPIRATION	30 JUNE 1970
CONTRACT AMOUNT	$198,967

CONSUMER & TECHNICAL PRODUCTS DIVISION
OWENS-ILLINOIS, INC
TOLEDO, OHIO
PHONE: (419) 242-6543, EXTENSION 33866

FORWARD

The work outlined in this semi-annual report was performed under Contract DAHC15 69 C 0303, ARPA Order 1441, and Program Code P9D10. The work was performed within the Consumer and Technical Products Division of Owens-Illinois, Inc., Toledo, Ohio and covers the period 30 June 1969 through 31 December 1969.

The principal investigator for the program is R. W. Beck while the program manager is H. A. Lee. This contract is administered by the Chief, Defense Contract Administration Services Office, Toledo, Ohio. Dr. R. A. Higgins, Director for Materials Sciences, ARPA, is the Contracting Officer's Technical Representative.

TABLE OF CONTENTS

LIST OF FIGURES

LIST OF TABLES

1. SUMMARY

The research goal of this program is to evaluate the radiation damage thresholds of neodymium doped glass laser materials and to ascertain the associated damage mechanisms. The research objectives are to:

1. Determine the relationship between active and passive damage threshold evaluations.
2. Relate the damage threshold to material homogeneity.
3. Evaluate damage threshold versus pulse width.
4. Determine the kinetics of output degradation at 20, 30, and 50 joules/cm^2 average intensity.
5. Coordinate with and furnish samples to the Naval Research Laboratory (NRL) for comparative evaluations.
6. Coordinate with and furnish samples to the National Bureau of Standards (NBS) for damage mechanish studies.

The principal test facility for this study is an oscillator-amplifier, Q-switched, laser system developed by O-I. A complete description of the test facility may be found in Section 2.

A summary of the activities during the work period 30 June 1969 to 31 December 1969 is as follows:

1. Six third amplifier rods, melted in platinum, were selected from three billets A, B, and C and actively tested for damage threshold. The damage thresholds varied from 12.8 to 31.1 joules/cm^2 peak intensity, with an average value for the six rods of 17.8 joules/cm^2. This test will serve as a reference from which further progress in the melting of laser glass in platinum may be evaluated.

2. Two, platinum melted, third amplifier rods have been life tested at 36 joules/cm^2 peak intensity. Damage to the rod output faces limited the number of shots to fifty and eighty-five respectively. The system performance did not degrade until the face damage became severe. The face damage was attributed to lenticular inclusions which formed within the rod during testing.

3. Life testing at 40 joules/cm^2 average intensity was attempted; however, surface damage to system components indicates that this level is presently unrealistic.

4. A sample of glass, suspected to have a large amount of platinum, was inspected with a microscope to determine the size, location, and type (crystal or agglomerate) of inclusions present. Sixteen inclusions, five microns or larger, were located, with twelve identifiable as crystals. When the sample was irradiated with 8 and 21 joules/cm^2 peak intensity, fifty and six hundred and fifty inclusions were formed respectively. Upon re-examination of the sample, the gross damage was found to be due to a high density (approximately 200/mm^3) of submicron size inclusions, whose identity has yet to be determined.

5. Oscillator and amplifier rods have been supplied to NRL for evaluation in the CCE VD 320 French laser system. The oscillator rod generated 3 joules in 30 nano-sec. with two-thirds of the French input. The second amplifier rod attained the French output with 40% of the pump energy for a 400 to 500 μ sec pump pulse. Gain measurements indicated a

5. (continued)

roll off of the output from ED-2 for high pumping levels and was attributed to a UV pump induced host absorption loss. Two second amplifier rods were found to damage at 15 joules/cm^2 peak intensity.

6. Kirtland results indicate that ED-2 does not exhibit a UV pump induced absorption loss.

7. Using the NRL and Kirtland results, O-I gain measurements at 10×10^{-3} and 100×10^{-3} joule/cm^2 average input energy densities indicate that high energy pumping losses are due to super-radiance and/or upper level absorption. At the present time we favor the super-radiance loss mechanism.

8. A 1.5 in. by 1.5 in. by 12 in. sample of platinum melted laser glass has been supplied to NBS for a statistical damage threshold study. Forward scattering measurements have been found to be insensitive for the detection of platinum.

2. DESCRIPTION OF TEST EQUIPMENT

2.1 High Peak Power Laser System

The principal test facility for the damage threshold studies is a Q-switched, oscillator-amplifier, Nd^{3+}: glass laser system. A schematic of the energy storage and discharge circuits associated with the system is presented in Figure 1. The storage network consists of six lumped capacitor-inductor units, with values of 325 μf and 100 μh respectively. The maximum energy storage is 5,850 joules at 6.0 KV for the oscillator unit and 4,060 joules per lamp at 5.0 KV for each of the amplifier units. This results in a total maximum system storage of 26,160 joules.

The optical configuration for the system appears in Figure 2. The oscillator is pumped with a single FX-95C-4 helical flashlamp while each of the first two amplifiers is pumped with double FX-95C-4 helical flashlamps. The third amplifier uses single lamp pumping. The rotating resonant reflector, Q-switched, oscillator will generate a maximum of 12 joules, full aperture, in a 40 nanosec pulse. To enhance the system beam uniformity an 11 mm major axis elliptical aperture is placed after the oscillator output mirror. The beam is then expanded and recollimated by a 1.5 X telescope, after which it passes through the three amplifier stages. Elliptical apertures with 16.5 mm major axes are placed on the input faces of amplifiers one and two to keep the beam from striking the sidewalls of the amplifier rods and to lessen the probability for damage to the output faces of the amplifiers. The average energy density within the system is sampled both at the

BLANK PAGE

FIGURE 1

CAPACITOR BANK SCHEMATIC

ALL CAPACITORS 65 M.F.D. 6.0 KV

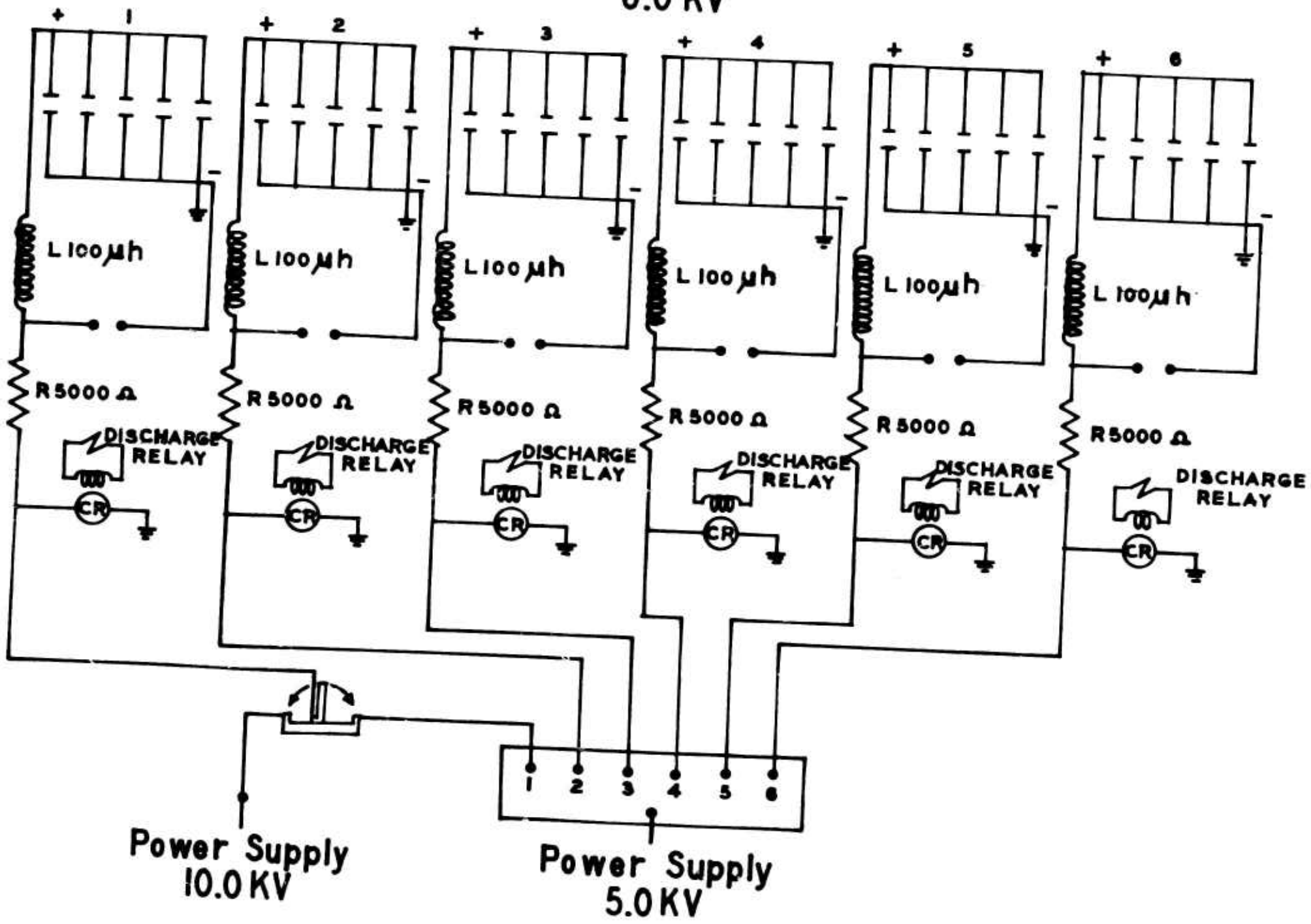

FIGURE

OSCILLATOR A
OPTICAL CONFI

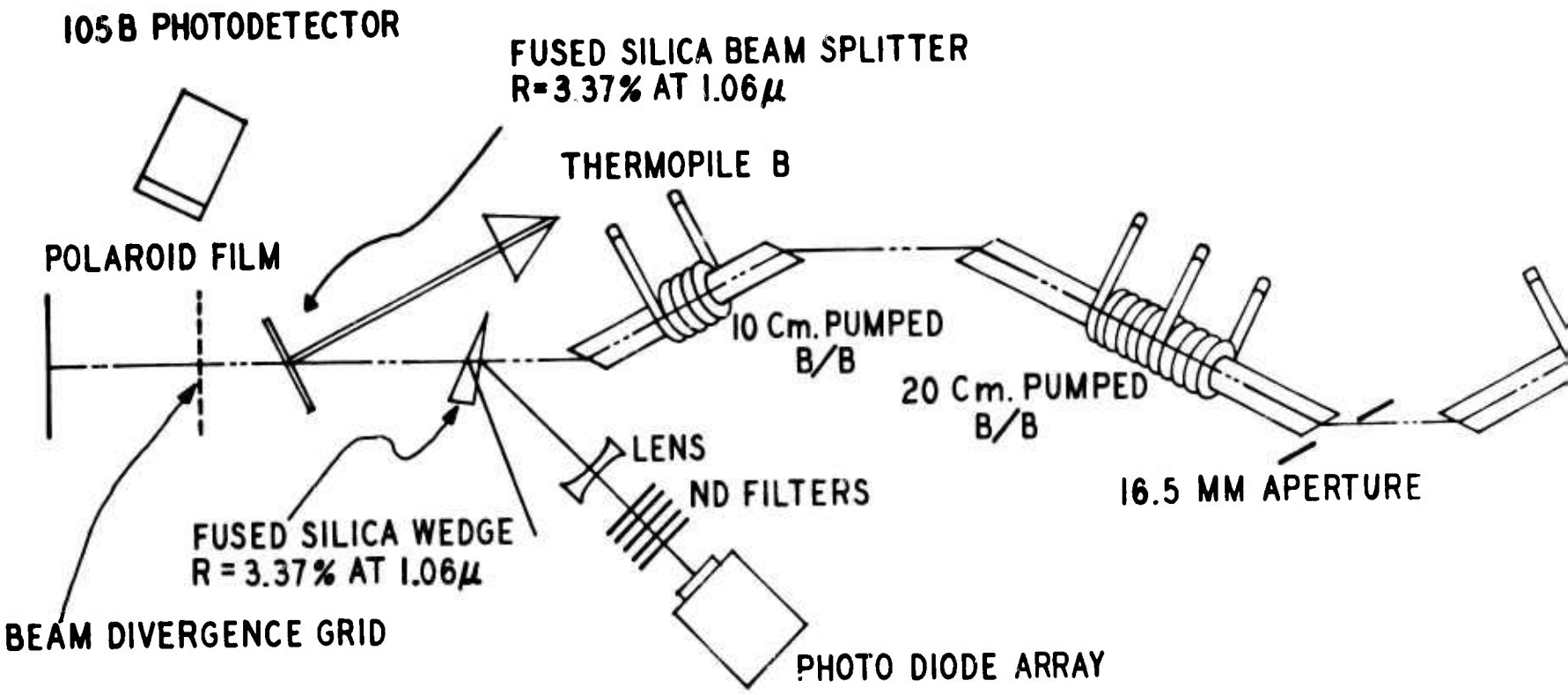

FIGURE 2

LATOR AMPLIFIER
L CONFIGURATION

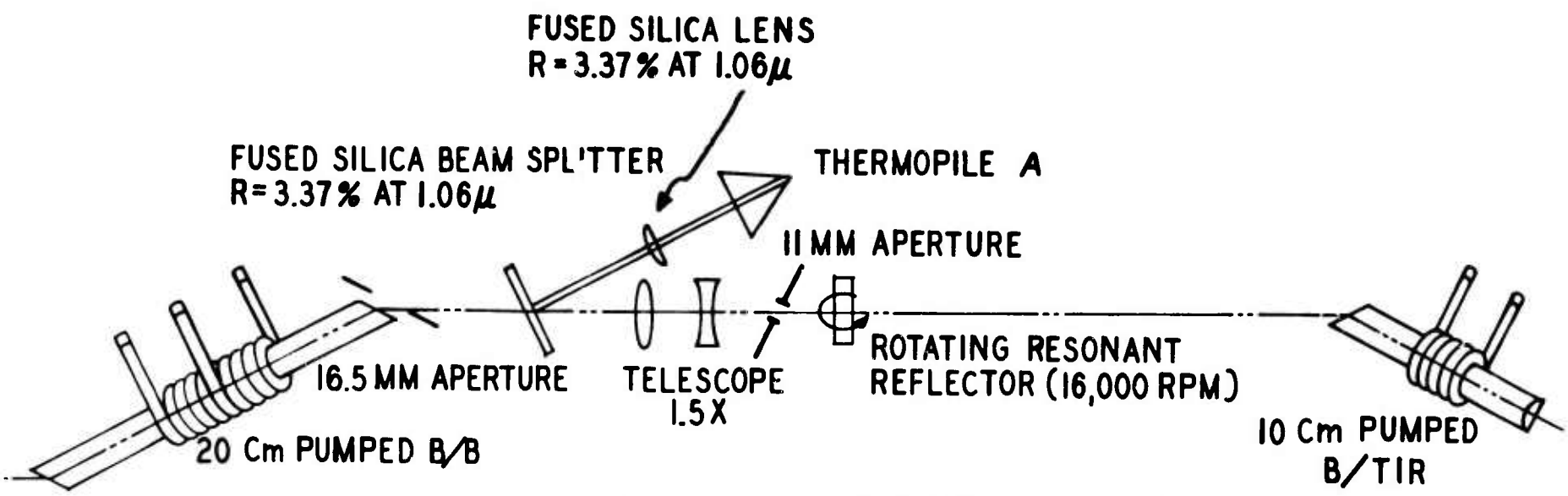

E

WATER COOLED SYSTEM (RODS & LAMPS)
ALL LAMPS FX-95C-4 HELICAL
ALL RODS 19 MM DIAMETER
LAMPS COUPLED TO RODS WITH SILVER REFLECTORS

B

2.1 (continued)

input and the output of the amplification stage. The sampling factor for both the input and output is 0.0619. The energy is monitored with TRG thermopiles and recorded on milli-volt strip chart recorders. The oscillator section of the system can be converted to a Beckman and Whitley air-driven TIR, rotating at 60,000 rpm, or to a Kerr Cell for shorter pulse generations.

Active damage threshold is observed in the third amplifier stage. The occurrence of damage is marked by the presence of a visible inclusion with the sample illuminated with a microscope lamp. Passive damage tests are performed on unpumped samples. The dependence of damage threshold on material homogeneity is evaluated by mapping the number, size and type (crystal or agglomerates) of inclusions within the sample prior to irradiation. After irradiation, the sample is remapped and any changes are noted in the number and size of the inclusions present. A Leitz Ortholux microscope with a 2 to 3 μ particle size resolution is available for this purpose.

2.2 Beam Divergence Measurements

The system beam divergence is determined by burning exposed Polaroid film, placed 100 cm behind a pinhole grid. A schematic of the grid is shown in Figure 3. A 1 mm change in the diameter of a ring of grid holes at the film surface represents a 1 milliradian full angle change in beam divergence. The system typically has a slightly better beam divergence in the direction across the

FIGURE 3

BEAM DIVERGENCE GRID

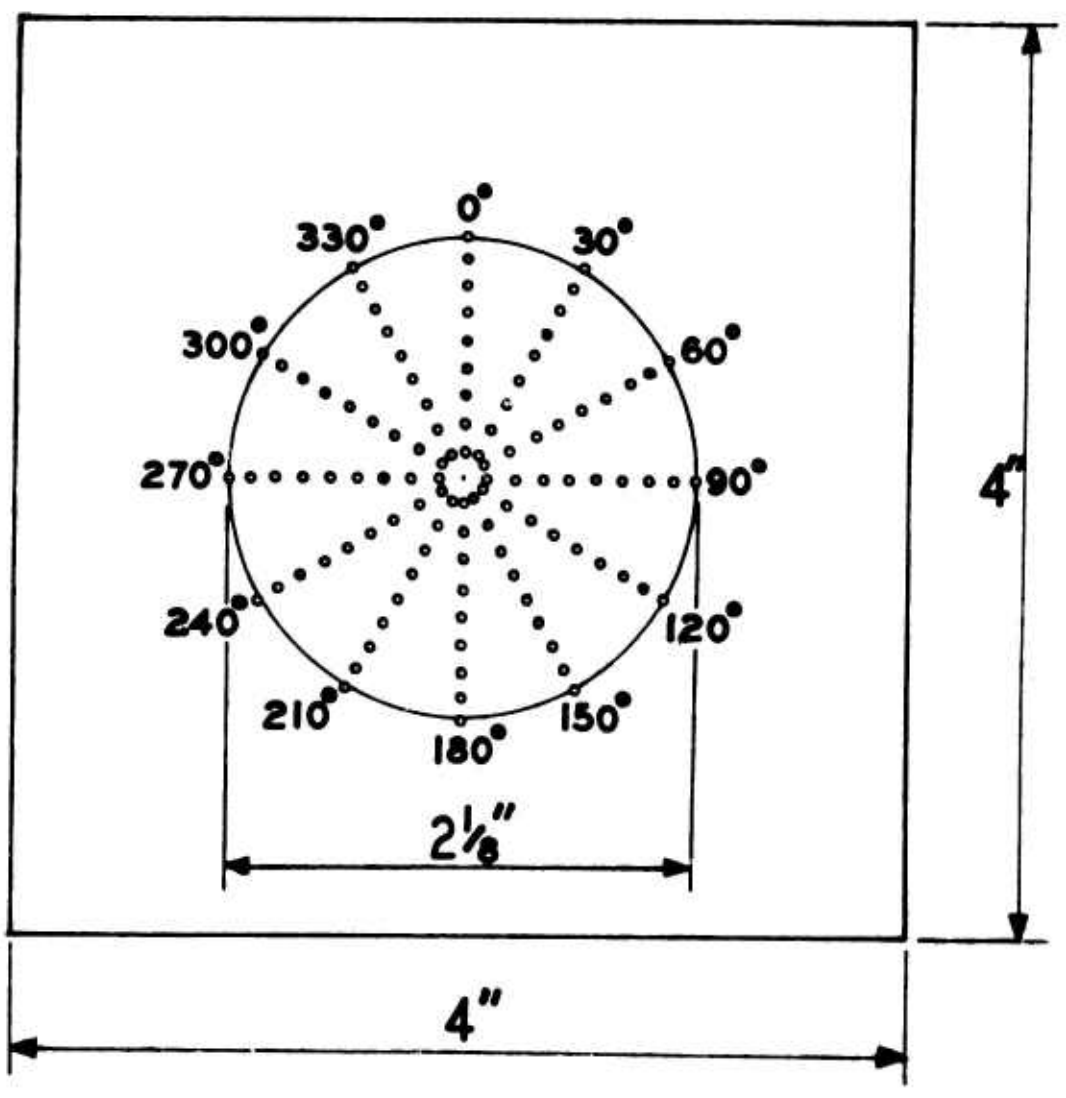

2.2 (continued)

TIR roof edge than along the TIR rod edge. For an oscillator cavity length of 135 cm the vertical and horizontal full angle beam divergences of the system for a 30 joule output are 0.5 and 1.5 milli-radians respectively and for a 60 joule output are 1.0 and 2.0 milli-radians respectively.

It should be noted that the insertion of the grid into the system produces enough feedback to severely broaden the laser emission pulse width. Because of this effect, continuous beam divergence monitoring is not possible and the grid is only inserted intermittently for beam divergence measurements.

2.3 Output Pulse Width

The pulse width of the laser emission is measured with a TRG 105B photodetector and a 519 Tektronix oscilloscope. The signal is picked up by viewing the Polaroid film target. The oscillator typically generates a 40 nano-sec pulse. When the oscillator signal is amplified to approximately 60 joules the system pulse broadens to 50 nano-sec.

2.4 Beam Profile Measurements

The device used to measure the beam profile is a United Detector photo diode array consisting of thirteen photo diodes in the form of a cross. The diodes are spaced on 0.150 inch centers and each diode is 0.080 inch in diameter. Each diode is part of a separate channel consisting of a light sensing circuit, an emitter follower transistor stage, and an RC storage network.

2.4 (continued)

A schematic of the channel circuitry is shown in Figure 4. The incident 1.06 micron radiation causes current to flow in the sensing circuit and a voltage to be generated at the output of the circuit. This signal is applied to the base of the transistor which charges the capacitor in the emitter circuit of the transistor. The response time of the sensing circuit is 8 nano-sec. for a 50 volt bias, and the RC time constant of the storage circuit is 270 nano-sec. The sensitivity of the diodes is greater than 0.5 μ amp/μ watt. The storage capacitor is a very low loss type. The 50 volt bias is maintained with a Kepco regulated DC power supply while the capacitor voltages are measured with a high input impedance Kiethley 610 A electrometer. A photograph of the diode array is presented in Figure 5.

The array is calibrated with uniform laser energy and the capacitor voltages are normalized to diode number four to provide relative profile measurements.

The placement of the photo diode array in the system is shown in Figure 2. The distance from the output end of the third amplifier rod to the array is nominally 50 cm. The negative lens expands the output pattern to fill the array as shown in Figure 6.

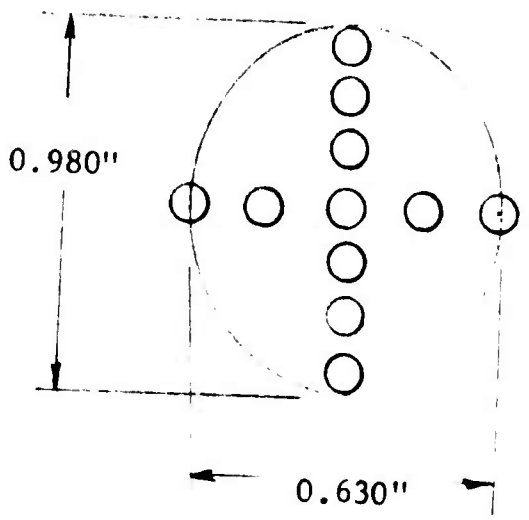

Lasing Pattern at
Diode Array Surface

Figure 6

FIGURE 4

DIODE ARRAY CIRCUIT (ONE CHANNEL)

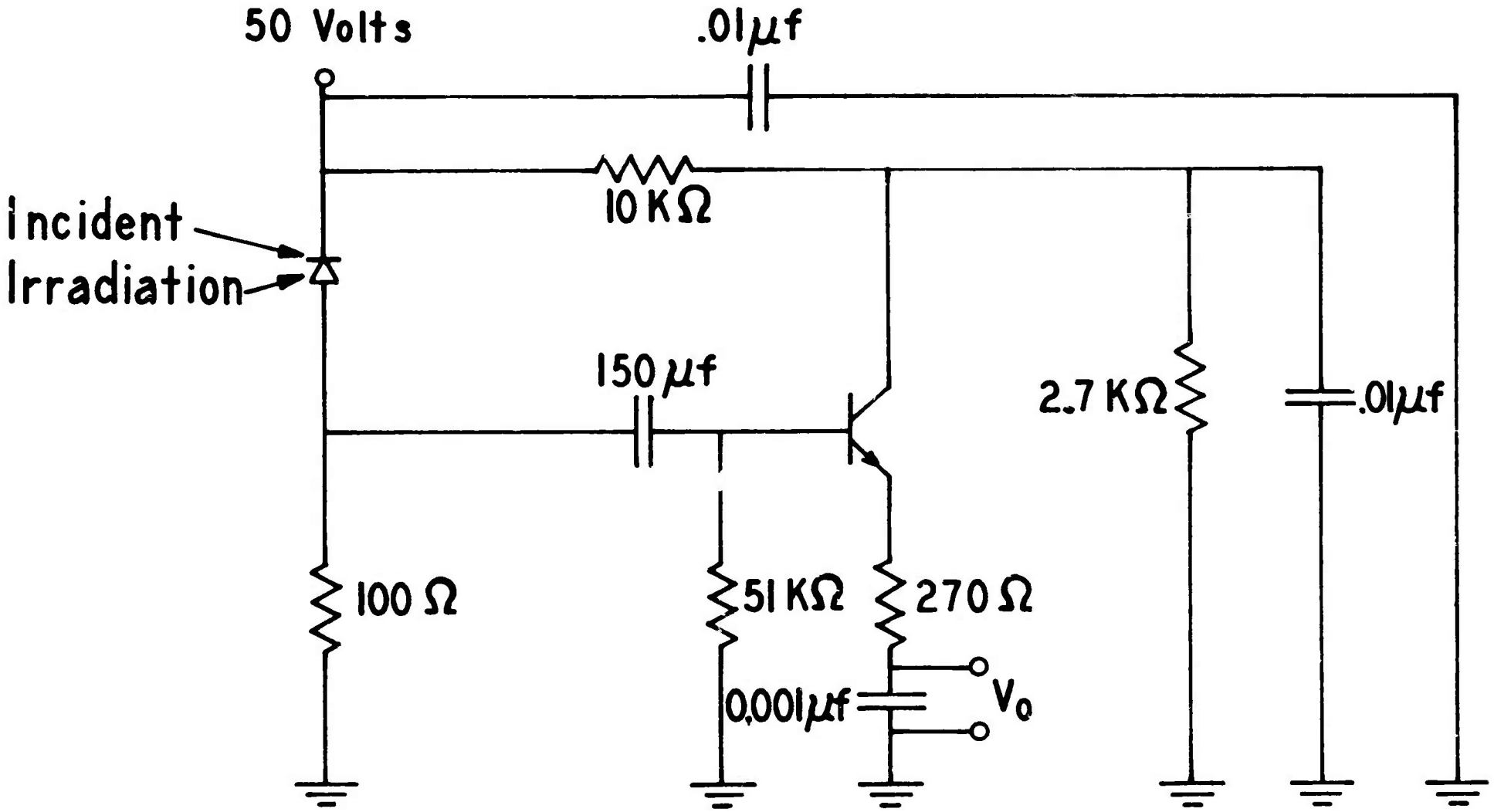

DIODE ARRAY

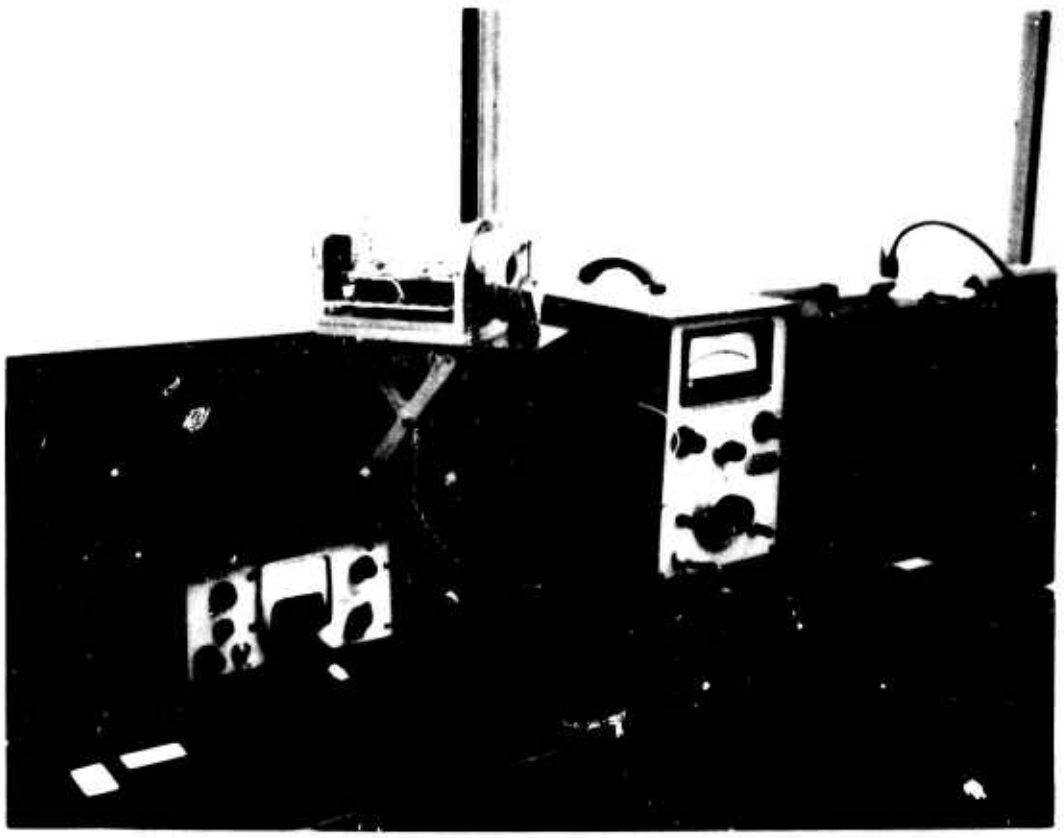

FIGURE 5

2.4 (continued)

The horizontal set of diodes (diodes 1 through 7) is positioned to read along the direction of the oscillator TIR roof edge while diodes 8 through 13 sample the beam in the direction perpendicular to the roof edge. A typical set of voltage readings obtained with the system running at an average of 31 joules/cm^2 output intensity is presented in Figure 7.

To convert voltage readings to energy densities (joules/cm^2) a computer program was written which integrates the volume contained by a surface generated from the eleven voltage measurements. This volume is then divided by 2 cm^2, which represents the area of the circular cross section of the beam within the amplifier rods, and is equated to the measured average energy density. The resulting energy density corresponding to one volt is then applied to each measured capacitor voltage, completing the conversion to energy densities.

The generation of a surface from the eleven voltage measurements proceeds as follows. The diodes are considered to be points and to be equally spaced along the X and Y directions of the 2 cm^2 circular cross section of the beam, as shown in Figure 8. Off axis voltage values are generated by drawing imaginary circles through diodes 10 and 11, and 9 and 12, with diode 4 as the center. Voltage values are assigned to the intersections of these circles with the X axis at points a, b, c, and d by assuming a linear relationship between the measured voltages on either side of the particular intersection. Voltage values along the circular arcs

FIGURE 7

BEAM PROFILE DATA
31 JOULES/Cm² AVERAGE INTENSITY

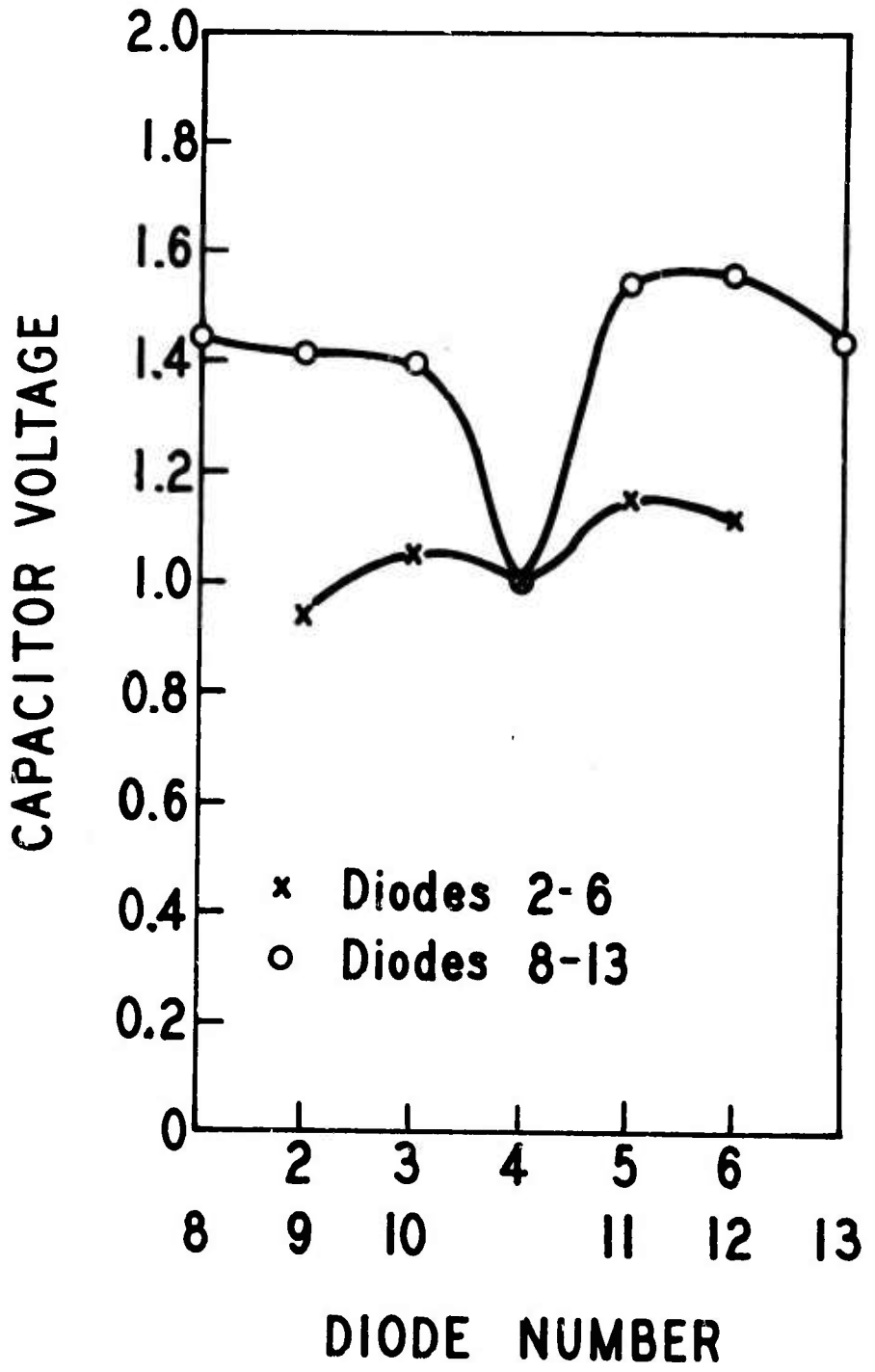

FIGURE 8

SURFACE GENERATION FROM MEASURED VOLTAGES

2 Cm^2 AREA

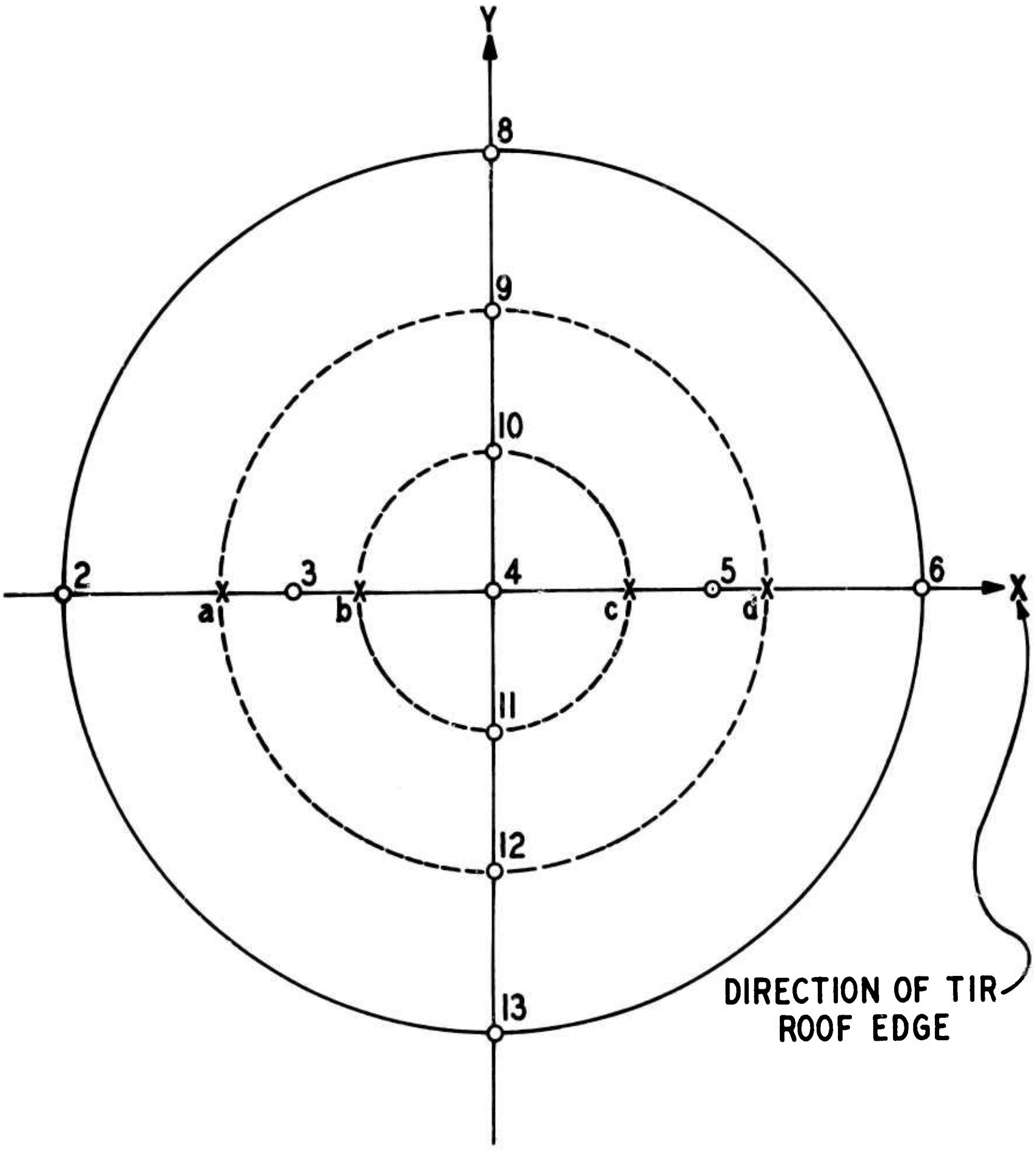

2.4 (continued)

within any particular quadrant are found by assuming a linear relationship between corresponding values on the X and Y axis. With these measured and generated values the volume integral is evaluated by summing volumes at five degree increments, first for the inner circle and then for the outer two annular sections.

Typical profiles for the system running at 14.3, 17.1, 22.4, and 30.7 joules/cm^2 average output intensity may be found in Figures 9 through 12.

A photographic paper that is sold by CGE and reported to be very sensitive to energy density is being obtained and will be compared with the values obtained with the beam profile device.

FIGURE 9

SYSTEM PROFILE
14.3 JOULES/Cm² AVERAGE INTENSITY

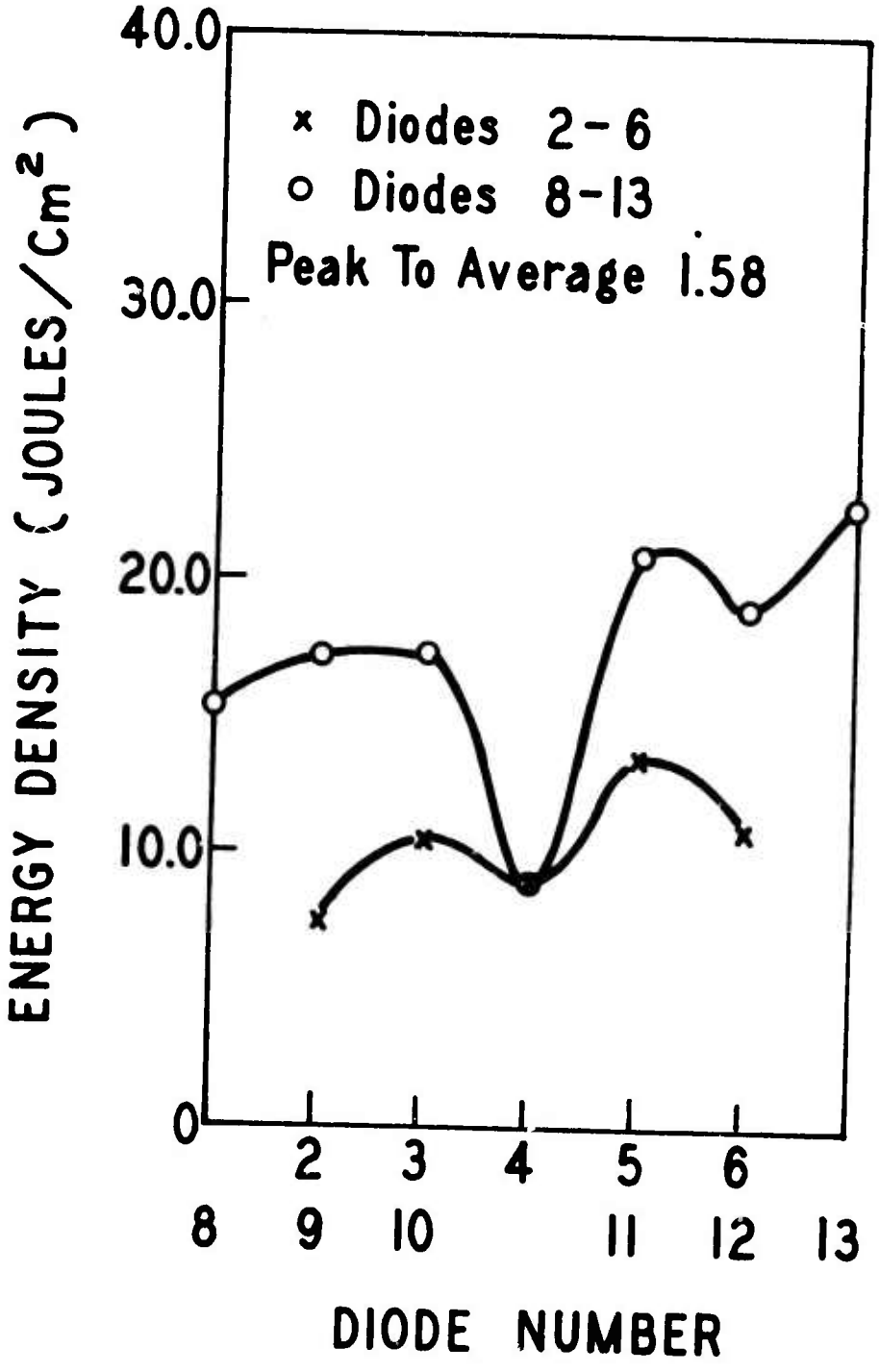

FIGURE 10

SYSTEM PROFILE

17.1 JOULES/Cm^2 AVERAGE INTENSITY

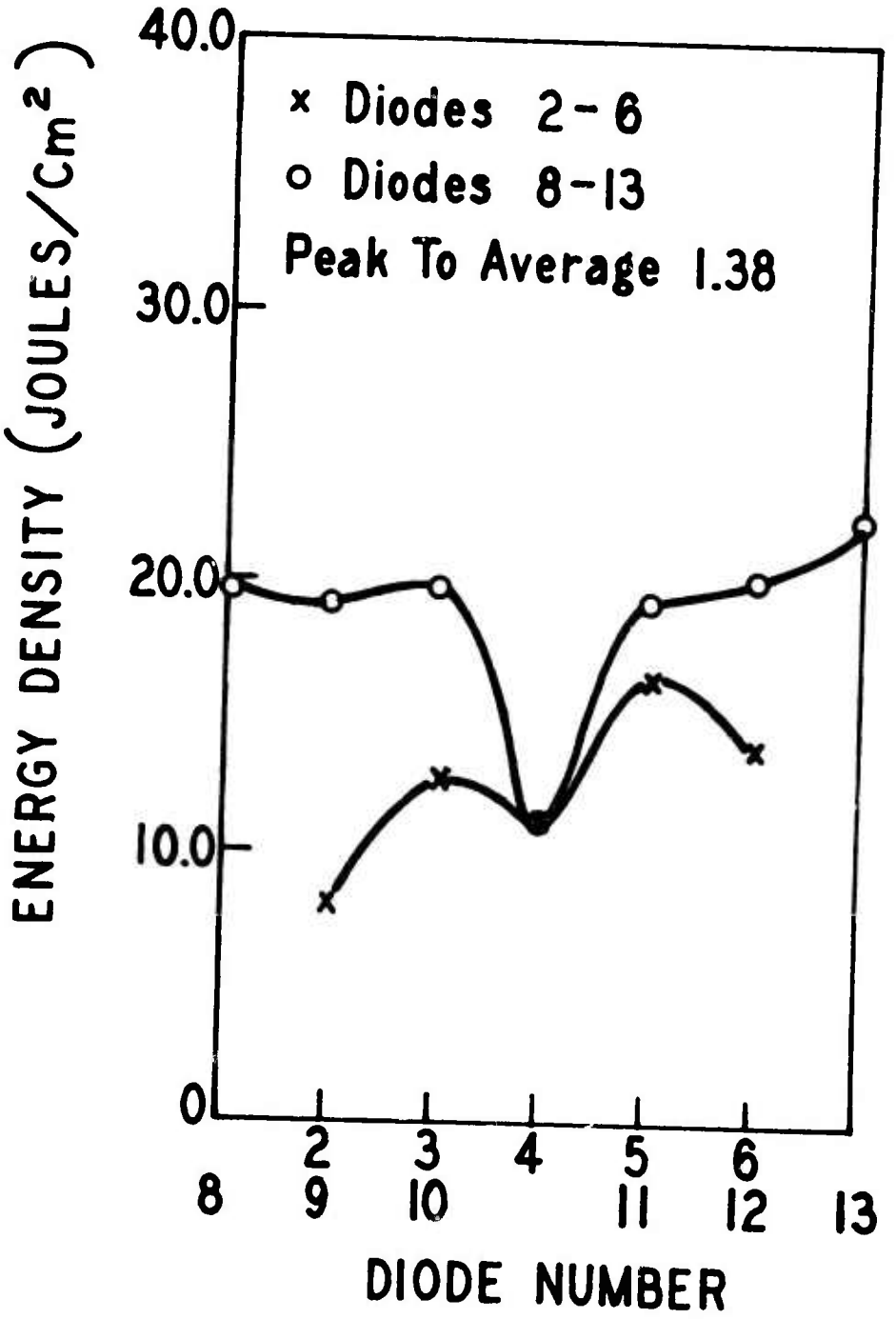

FIGURE II

SYSTEM PROFILE

22.4 JOULES/Cm^2 AVERAGE INTENSITY

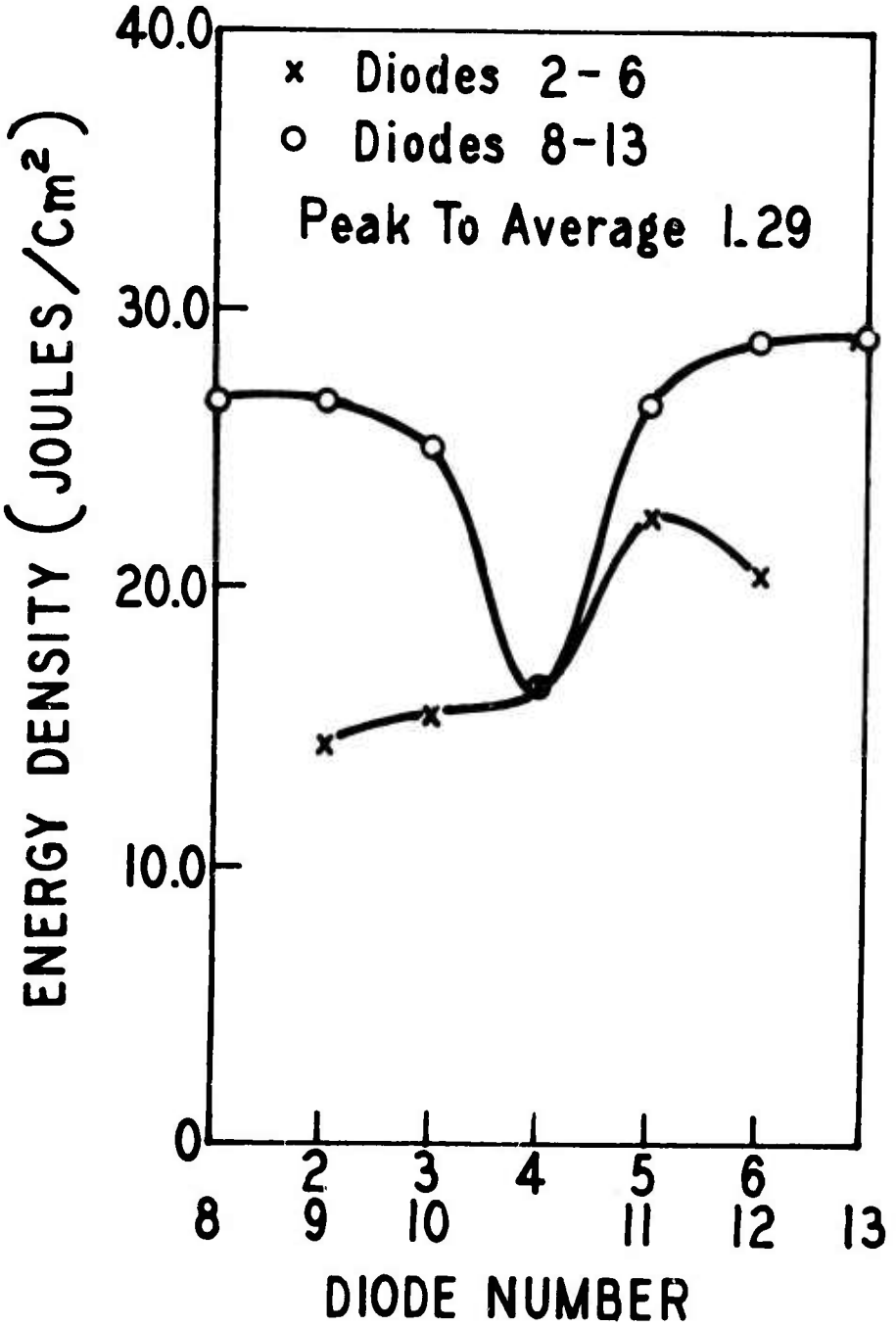

FIGURE 12

SYSTEM PROFILE

30.7 JOULES /Cm^2 AVERAGE INTENSITY

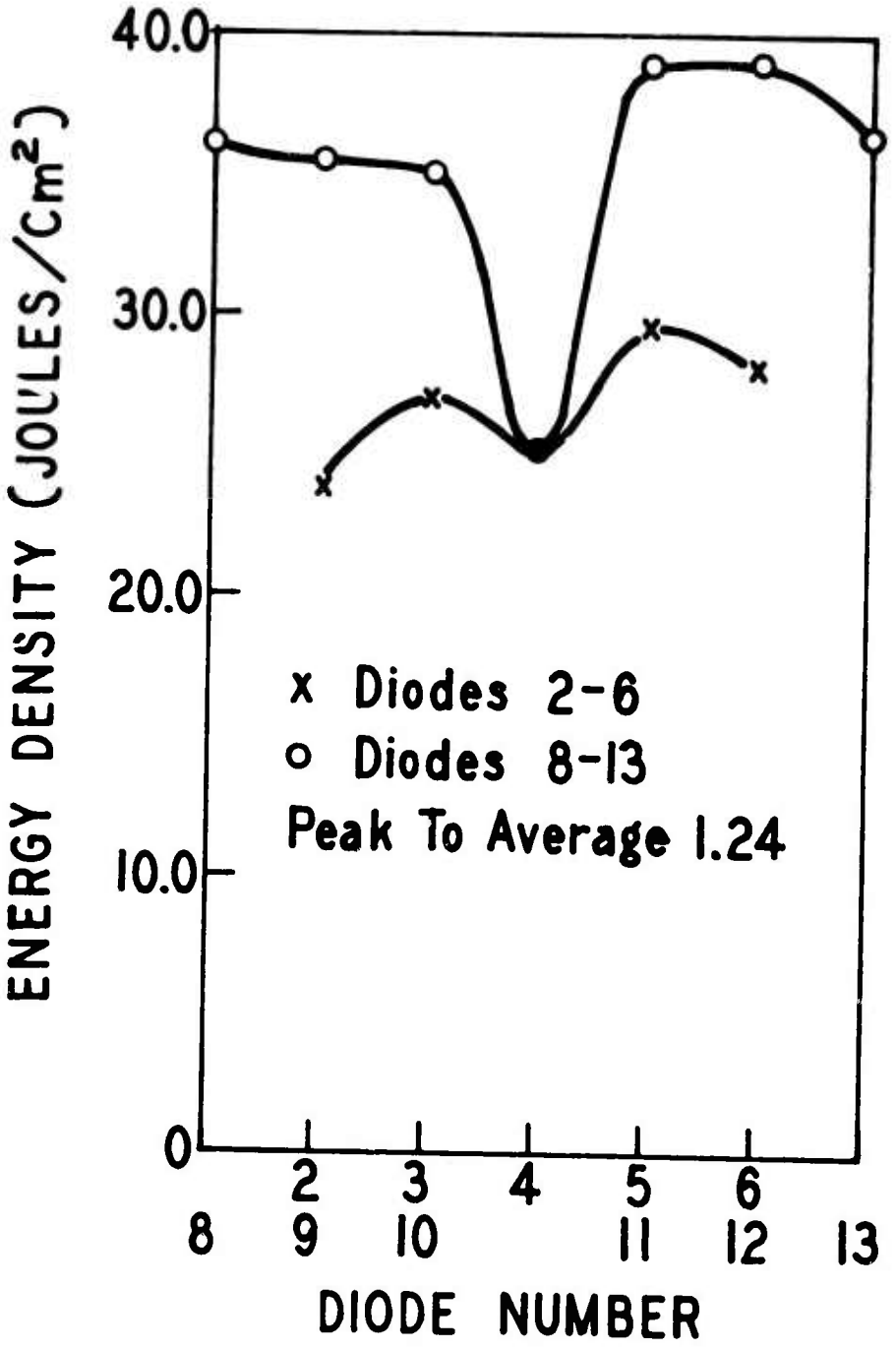

3. GAIN MEASUREMENTS

3.1 NRL Measurements

An ED-2 rod, 32 mm in diameter by 24.8 cm long, was evaluated in the second amplifier stage of the CGE VD320 laser system at NRL. The output energy density as a function of the pumping level is presented in Figure 13 for ED-2 immersed in water and for ED-2 and French glass immersed in water with 2.5 gm/liter of Potassium Dichromate added. The average input energy density to the second amplifier was 1.79 joules/cm^2, and the flashlamp pumping pulse was 1.0 msec. The French rod can be seen to have an almost linear input-output relationship, while the ED-2 rod exhibits considerable roll off for input energies above 12,000 joules. It is worth noting that the ED-2 rod reached the maximum output level of the French rod with 60% of the pumping input energy, and that this is with a 1.0 msec. pump pulse, which is much too long for ED-2 with its characteristic fluorescent lifetime of 300 usec. More recent work has shown that the maximum French output can be achieved at 40% of the input energy if the flashlamp pump pulse is reduced to 400 to 500 usec.

One inclusion formed during the series of shots at an estimated peak energy density of 15 ± 3 joules/cm^2.

Figure 14 shows the output energy density as function of the pumping level for an average input energy density of 5 joules/cm^2. The ED-2 rod is immersed in water only and again the flashlamp pump pulse is 1.0 msec. The rolling off of the output is

FIGURE 13

NRL CGE VD 320 ED-2 + FRENCH

SECOND AMPLIFIER RESULTS

(E in = 1.79 JOULES/Cm²)

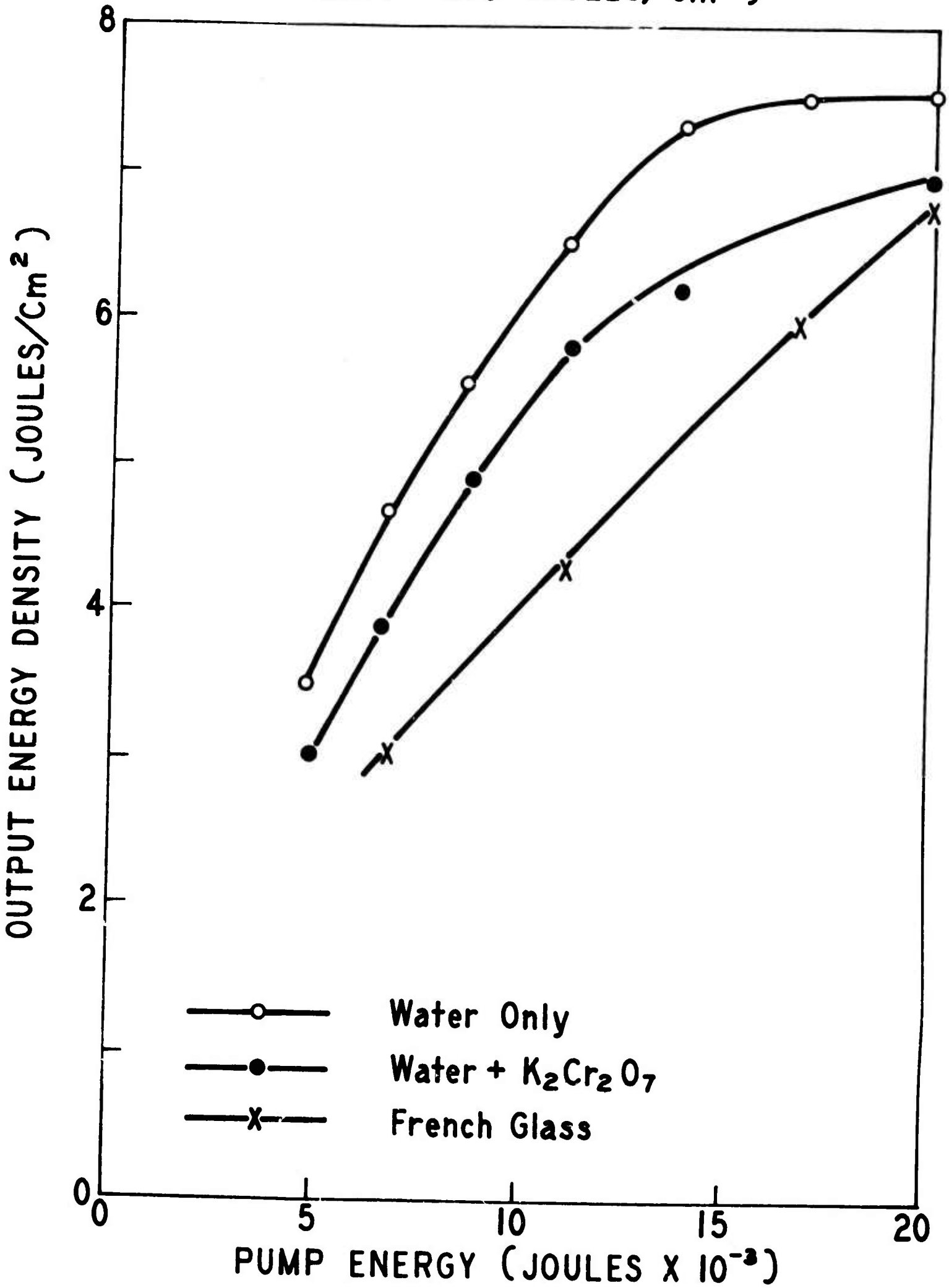

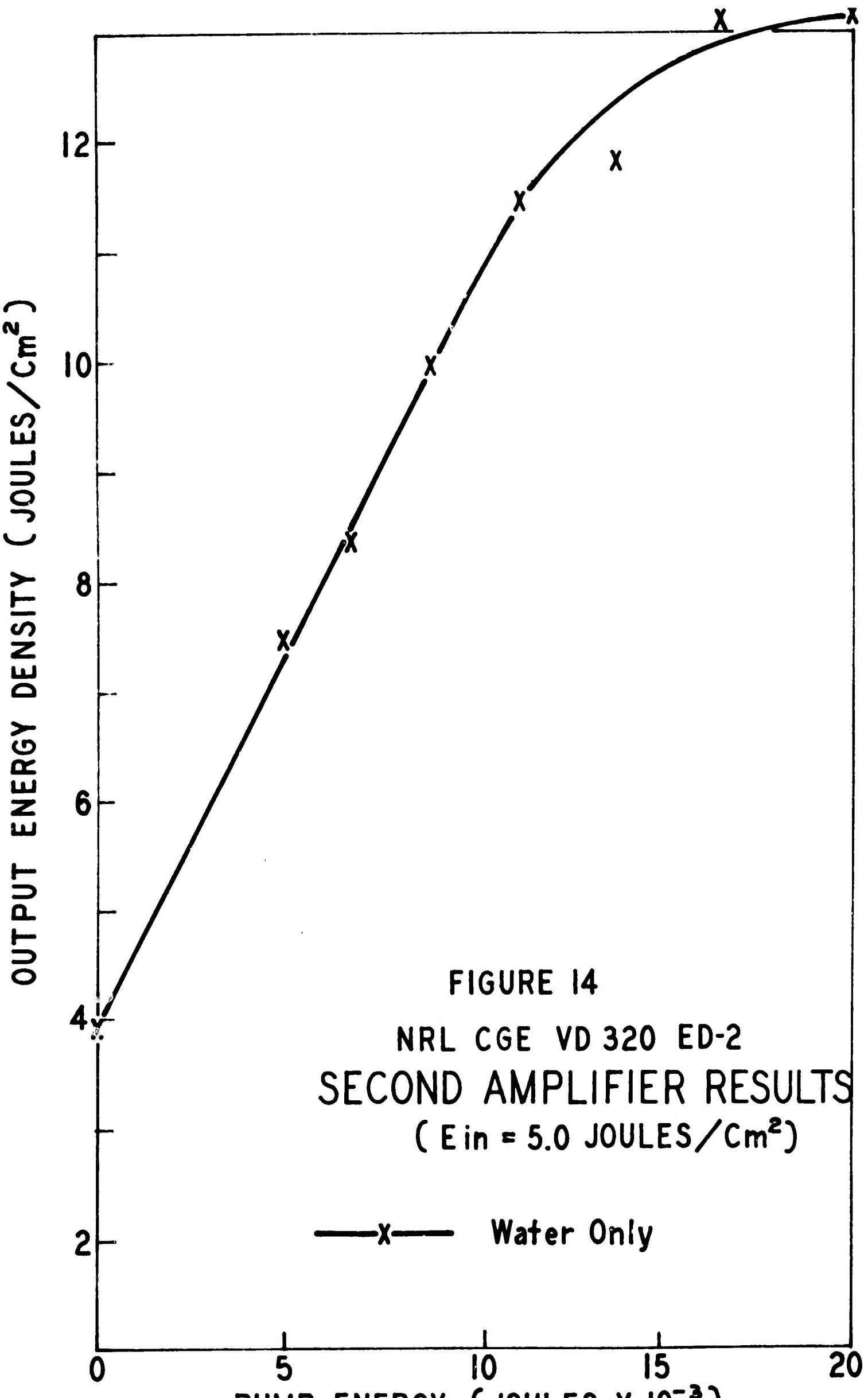
OUTPUT ENERGY DENSITY (JOULES/Cm²)
12
10
8
6
4
2
0
5
10
15
20
PUMP ENERGY (JOULES X 10⁻³)
FIGURE 14
NRL CGE VD 320 ED-2
SECOND AMPLIFIER RESULTS
(Ein = 5.0 JOULES/Cm²)
—X— Water Only

3.1 (continued)

again apparent for input energies above 12,000 joules. During this test series six additional inclusions formed in regions where the local peak intensities were between 16 and 24 joules/cm^2. Approximately 100 shots were run after the damage occurred, with no deterioration of the beam quality or system efficiency within the experimental error of $\pm$ 5%.

To illuminate the pronounced leveling off of the output of ED-2 at the higher input levels a sequence of tests was run in which the input pump level was fixed, while the laser input energy density varied. These results are shown in Figure 15. The following expression, which extends the theory of Avizones and Grotbeck on saturable ruby amplifiers to four level systems, was fit to the experimental data for each pump level by allowing

$\sigma/h\nu$, ΔN, and α to vary

$$\frac{dE}{dx} = \Delta N \left[1 - e^{-\frac{\sigma E}{h\nu}} \right] - \alpha E$$

where

E = energy density (joules/cm^2) at some point x within the amplifying medium

ΔN = population inversion (joules/cm^3)

$h\nu/\sigma$ = saturation flux (joules/cm^2)

α = loss coefficient (cm^{-1})

The computer fits indicated that the loss coefficient was increasing with the pumping energy with a power between 1.2 and 1.35. An experimental measurement of the lamp intensity between 3400 $\mathring{A}$ and 4800 $\mathring{A}$ indicated that the instantaneous intensity at the point the

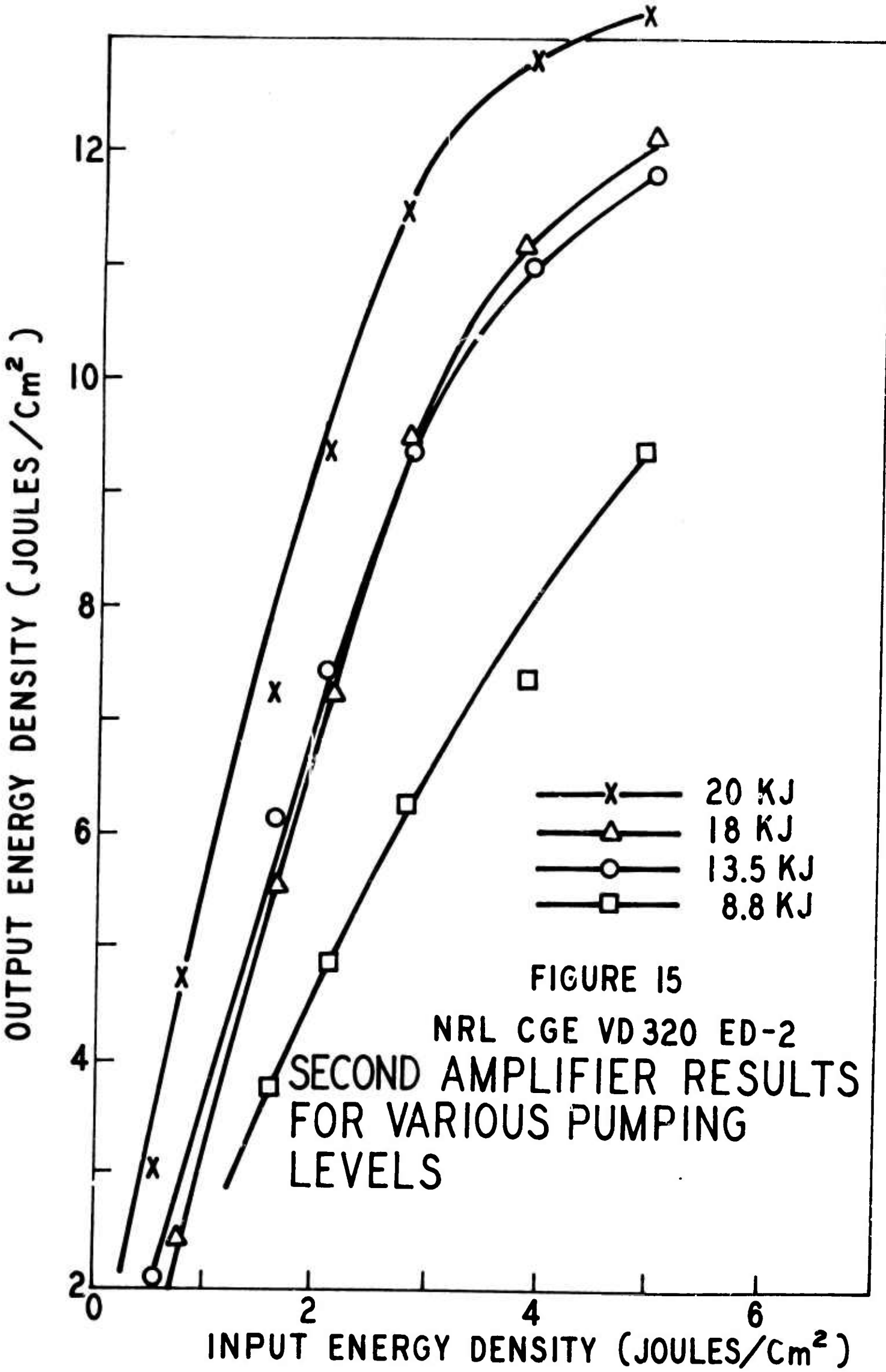

FIGURE 15

NRL CGE VD 320 ED-2

SECOND AMPLIFIER RESULTS FOR VARIOUS PUMPING LEVELS

3.1 (Continued)

laser was switched followed the power law, $K_1 E^{1.24}$, while the integrated energy from the start of the pulse to the point of Q-switching followed the power law $K_2 E^{1.325}$. This suggests a host UV pump induced absorption. Further work is planned to determine the mechanism of the absorption as well as its lifetime.

3.2 Kirtland Measurements

To evaluate the significance of the host UV pump induced losses proposed by NRL, the transmission of an ED-4 rod to 1.06 micron radiation versus the pumping level was determined at Kirtland. The transmission was found to be independent of the pumping level and thereby provides a strong argument against a transient UV induced host absorption in ED-2.

3.3 O-I Measurements

In light of the NRL and Kirtland results, gain measurements have been obtained for the first amplifier of the O-I oscillator-amplifier system for input energy densities of 10×10^{-3} and 100×10^{-3} joules/cm^2. The setup for the gain measurements is shown in Figure 16 and the experimental results may be found in Figures 17 and 18. In Figure 17, error bars indicating the maximum and minimum values obtained have been included for two data points which deviate appreciably from the fitted curve. It is significant to note that a severe roll off of the gain is not apparent for the pumping energies considered, although, as will be shown later, some roll off is present.

FIGURE 16

O-I GAIN MEASUREMENT SETUP

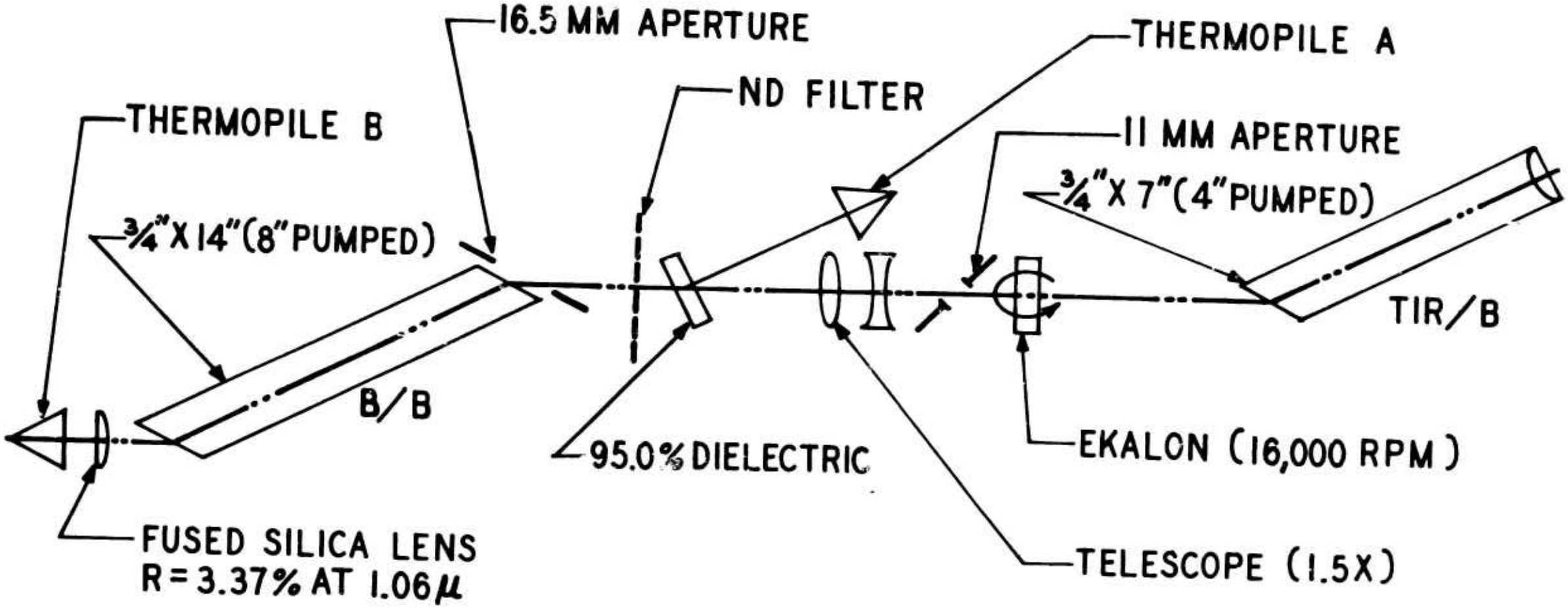

FIGURE 17

O-I GAIN RESULTS

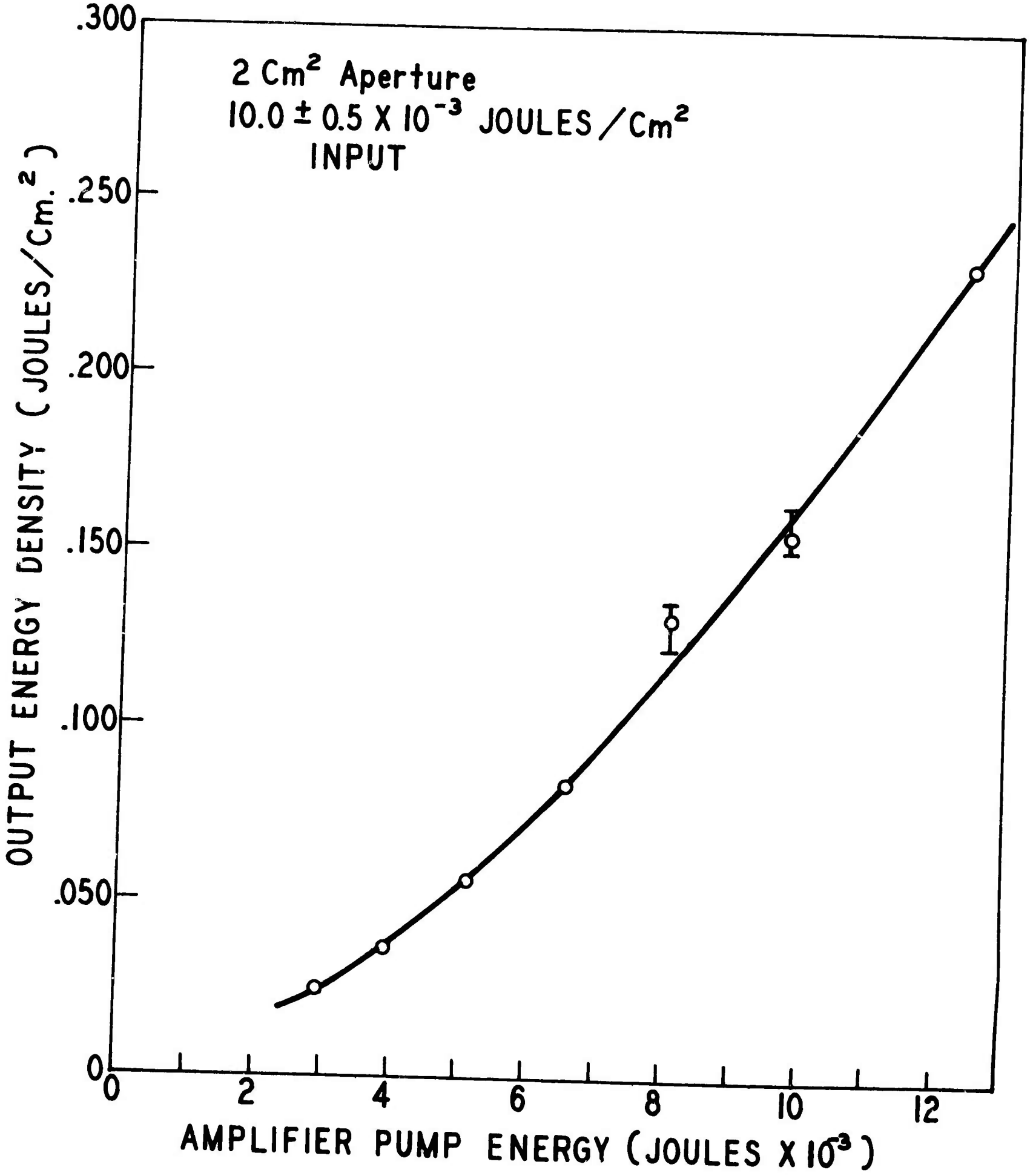

FIGURE 18

O-I GAIN RESULTS

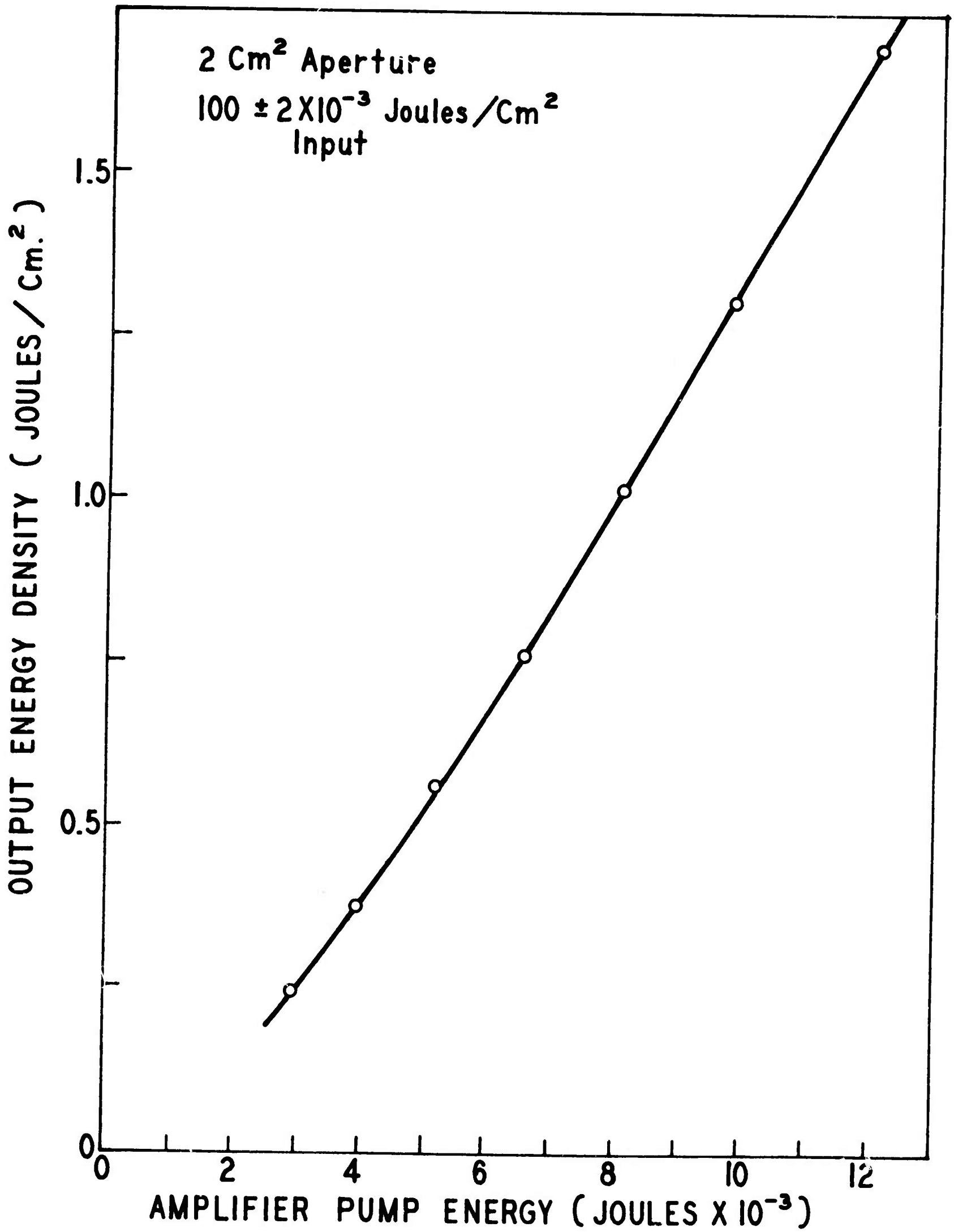

3.3 (continued)

To account for deviations of the experimental gain data from the aforementioned modified Avizonis and Grotbeck theoretical amplifier energy transport expression, computer solutions of the expression were generated for the following experimental conditions:

$$\sigma/h\nu = 0.16 \ m^2/joule$$

$$\alpha = 0.005 \ cm^{-1}$$

$$x = 20.3 \ cm$$

$$E_{in} = 10 \times 10^{-3} \text{ and } 100 \times 10^{-3} \ joules/cm^2$$

Because of the Kirtland results, for this analysis α was not allowed to vary, and any deviations of the experimental results from the theoretical model were absorbed by formulating the following expression for ΔN:

$$\Delta N = \frac{KE_p}{V}$$

where

K = fraction of the pump energy which contributes to inversion

E_p = flashlamp pumping energy

V = volume of the amplifier rod being pumped (57.9 cm^3)

The computer generated solutions which express energy density output ($joules/cm^2$) versus population inversion may be found in Tables 1 and 2 and Figures 19 and 20. To determine the value of K for each pump level which matches the theoretical solution to the experimental data, the energy density output for each pump

TABLE I

$\sigma/h\nu$ = 0.16 cm^2/joule x 20.5 cm

α = 0.005 cm^{-1} E_{in} = 10 x 10^{-3} joules/cm^2

Δ N	ENERGY DENSITY OUT
0.0	0.009
0.1	0.012
0.2	0.017
0.3	0.024
0.4	0.033
0.5	0.045
0.6	0.063
0.7	0.086
0.8	0.119
0.9	0.163
1.0	0.224
1.1	0.307
1.2	0.419
1.3	0.571
1.4	0.773
1.5	1.042
1.6	1.394
1.7	1.848
1.8	2.423
1.9	3.136
2.0	4.000

TABLE 2

$\sigma/h\nu$ = 0.16 cm^2/joule x = 20.3 cm

α = 0.005 cm^{-1} E_{in} = 100 x 10^{-3} joule/cm^2

Δ N	ENERGY DENSITY OUT
0.0	0.099
0.1	0.137
0.2	0.189
0.3	0.259
0.4	0.355
0.5	0.485
0.6	0.660
0.7	0.894
0.8	1.202
0.9	1.603
1.0	2.116
1.1	2.760
1.2	3.550
1.3	4.495
1.4	5.598
1.5	6.852
1.6	8.245
1.7	9.759
1.8	11.376
1.9	13.075
2.0	14.838

FIGURE 19

THEORETICAL GAIN
OUTPUT ENERGY DENSITY VS. DELTA N

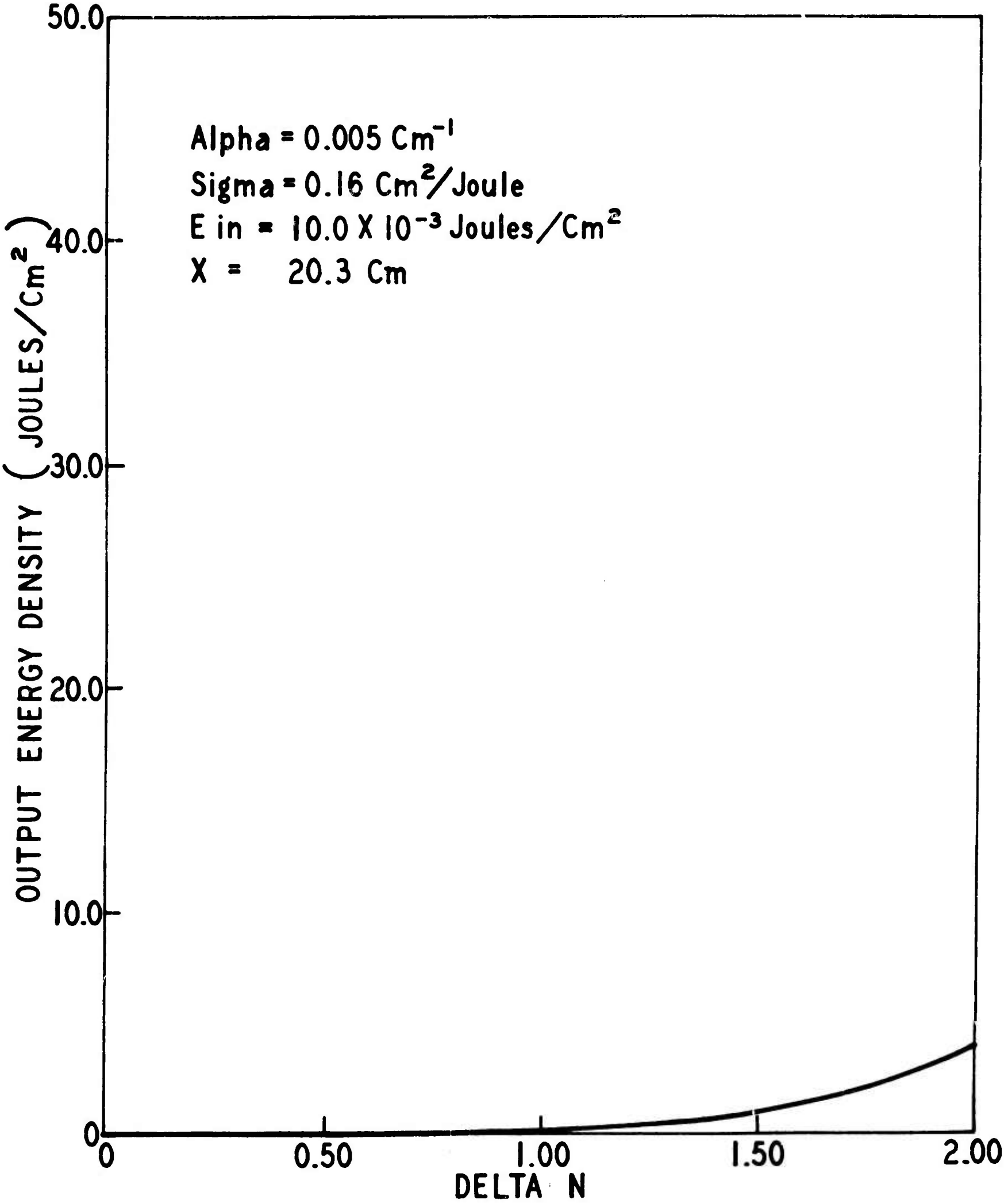

FIGURE 20

THEORETICAL GAIN
OUTPUT ENERGY DENSITY VS. DELTA N

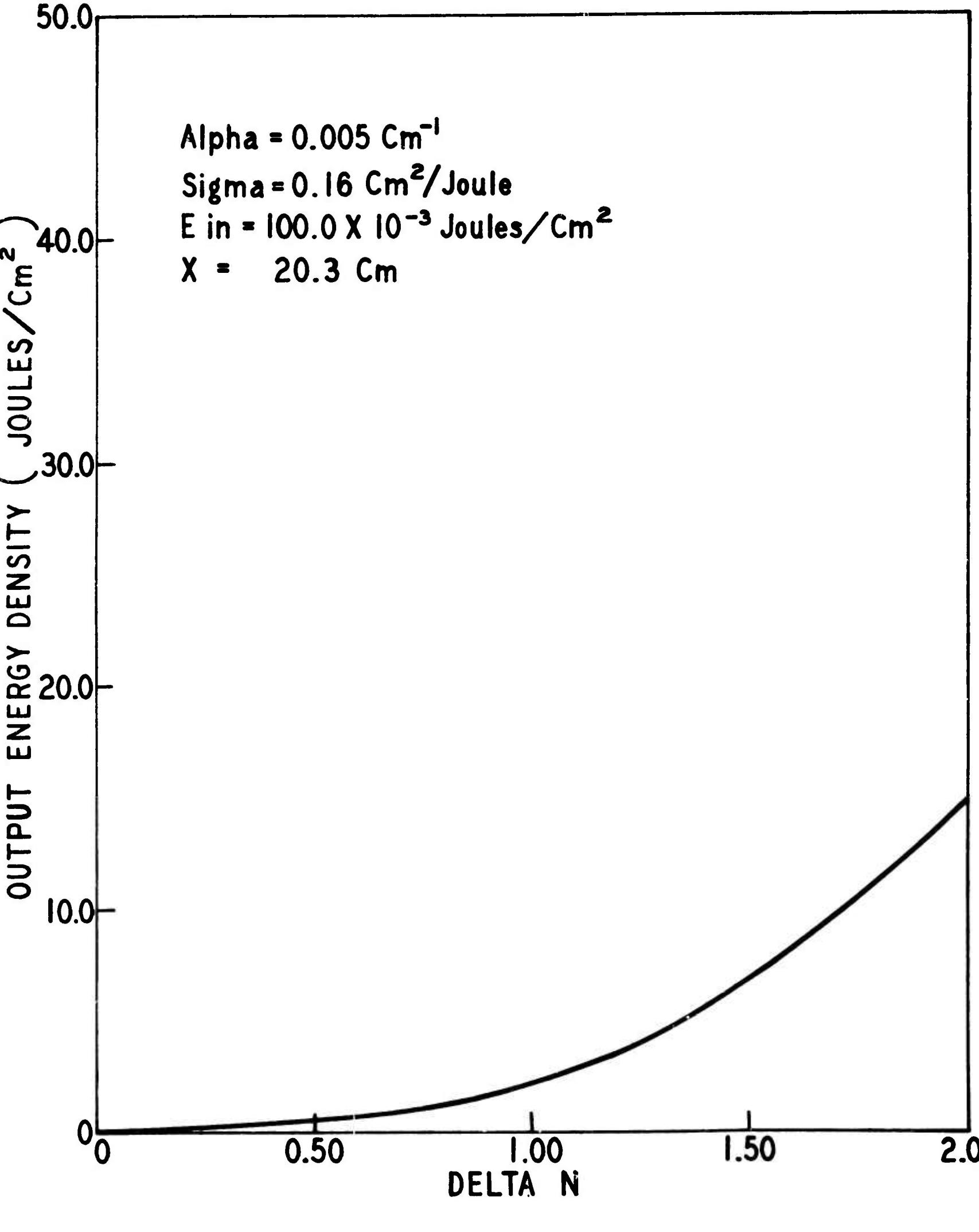

3.3 (continued)

level is equated to the stored energy density, presented in the Tables, required to achieve the output. The resulting K values are shown in Table 3. Since the K values should be independent of the laser input energy density to the amplifier, average values for the two sets of K values are presented in Table 4. The fraction of the pump energy which contributes to inversion is clearly not a constant and generally decreases with increasing pump energy.

A factor which could contribute to a variation in K with the pumping level would be the lamp spectral shift to shorter wavelengths with increased pumping energies. This could have a twofold effect. First, the percent of the total energy emitted within the pumping region may vary, and secondly, the percent of the energy emitted which is absorbed by the laser rod could change with the pump level. To evaluate the magnitudes of these two effects, the spectral characteristics of an FX-95C-4 amplifier pump lamp were evaluated with an EG+G Spectroradiometer between 4000 $\mathring{A}$ and 9200 $\mathring{A}$ for 3.0, 4.0, 5.0, and 6.0 KV. For each 50 $\mathring{A}$ interval, the energy absorbed by the laser rod was determined by considering the average path length of the pump light through the amplifier rod ($\frac{2}{\pi D}$ = 1.21 cm). The spectra and corresponding absorbed energies may be found in Figures 21 through 24. If the total area of the lamp emission is normalized to 5.0 KV, the percent variation of the total lamp output

TABLE 3

10×10^{-3} joules/cm^2

PUMP LEVEL	K
2920	0.0059
3980	0.0062
5200	0.0064
6580	0.0060
8125	0.0057
9830	0.0053
11700	0.0051

100×10^{-3} joules/cm^2

PUMP LEVEL	K
2920	0.0056
3980	0.0060
5200	0.0060
6580	0.0057
8125	0.0053
9830	0.0048
11700	0.0044

BLANK PAGE

TABLE 4

PUMP LEVEL	AVERAGE K
2920	0.0058
3980	0.0061
5200	0.0062
6580	0.0058
8125	0.0055
9830	0.0050
11700	0.0048

F

FX-95C-4 LAMP SPE

325 μf –

3

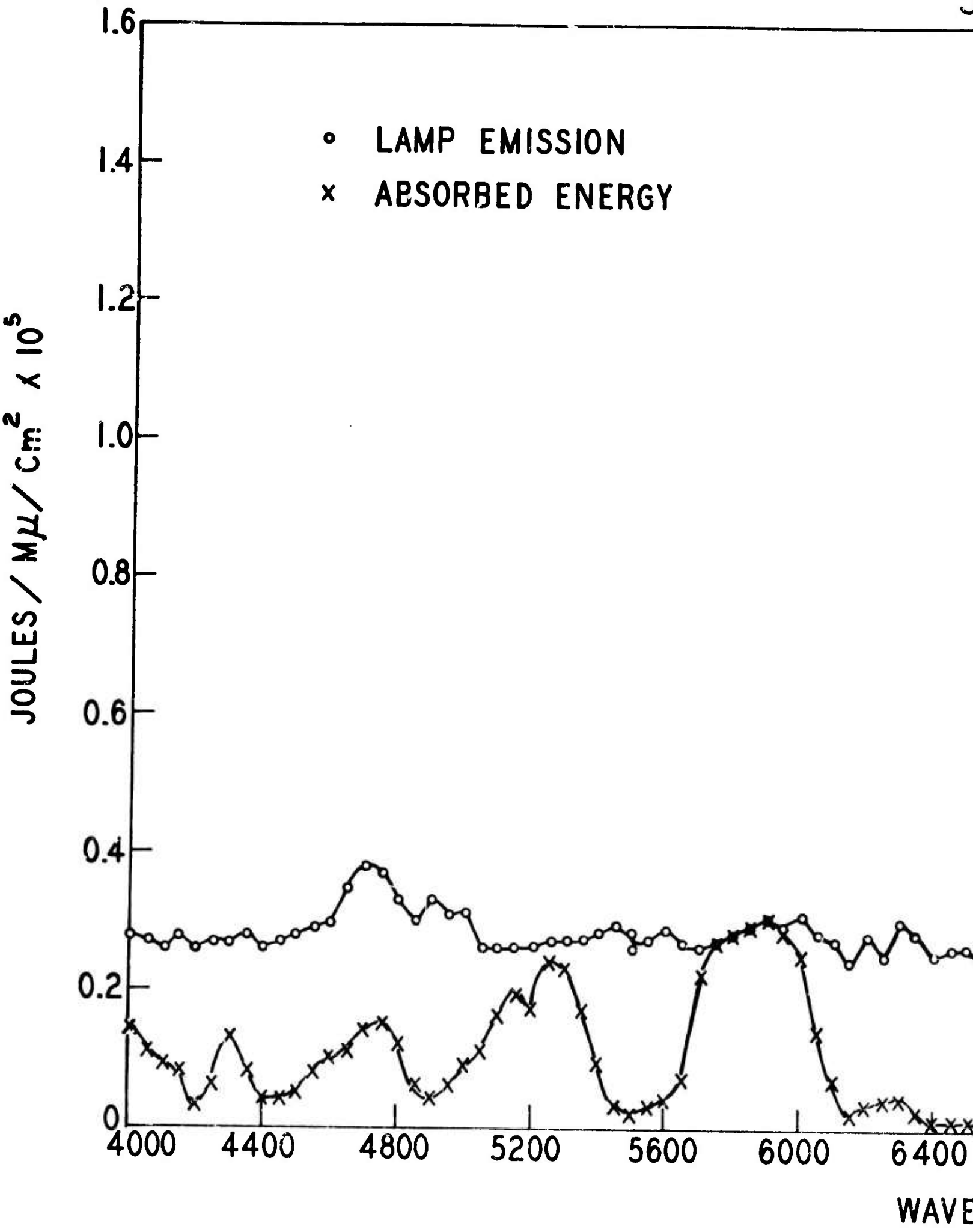

4

FIGURE 21

P SPECTRAL CHARACTERISTICS
5 μf - 100 μh LUMPED
3.0 KV

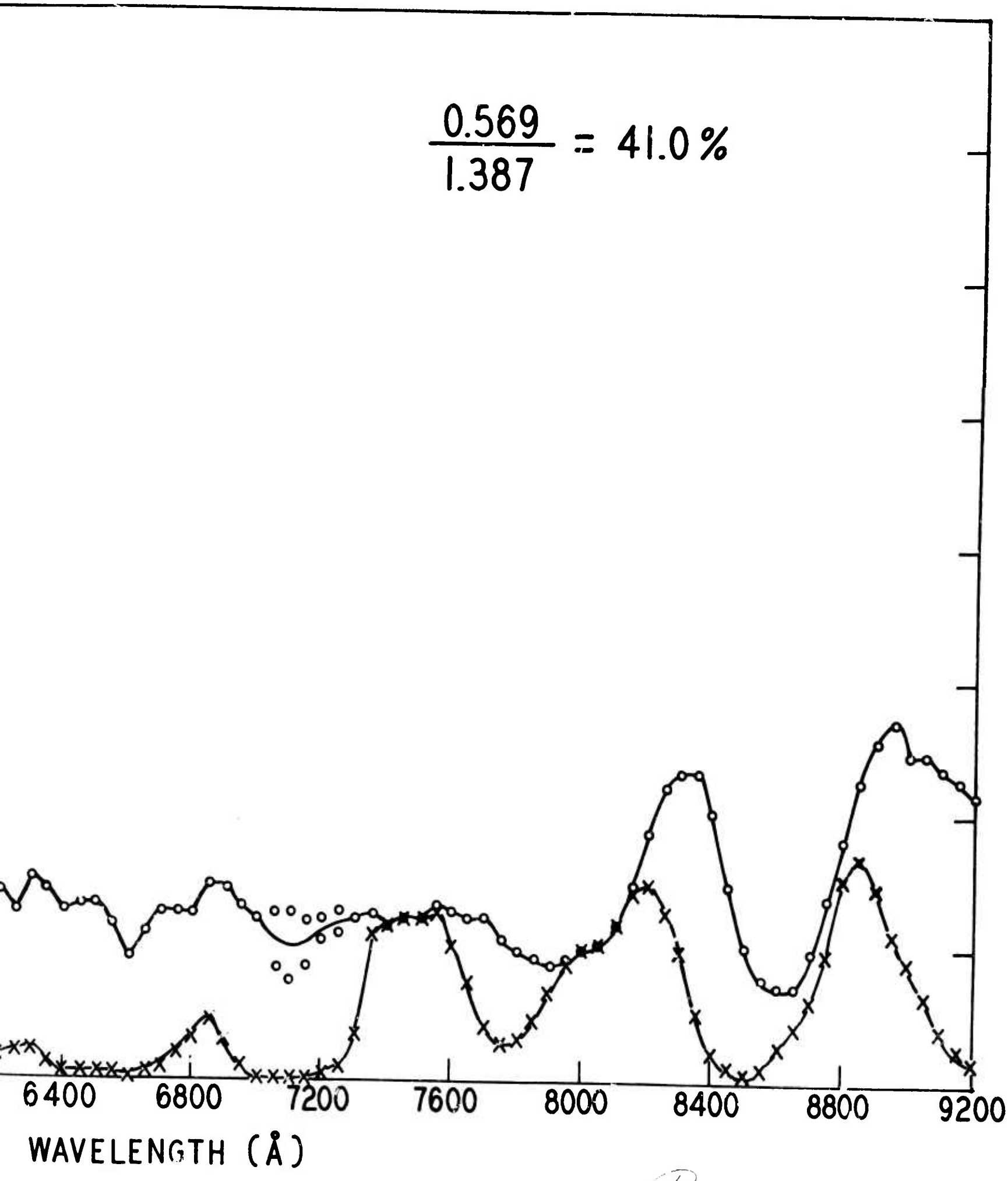

F

FX-95C-4 LAMP SPE

325 μf -

4

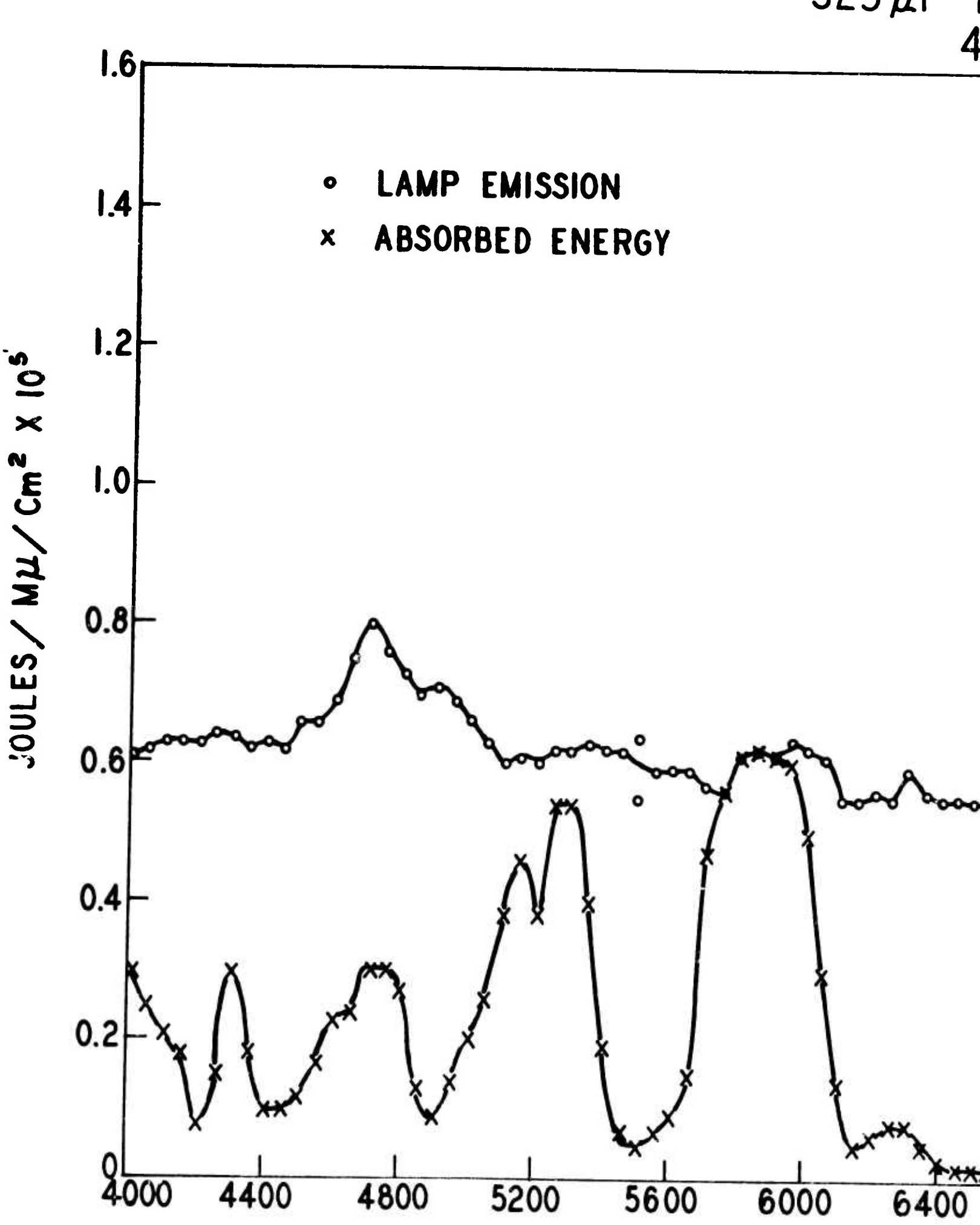

FIGURE 22

SPECTRAL CHARACTERISTICS

$5\,\mu f - 100\,\mu h$ LUMPED

4.0 KV

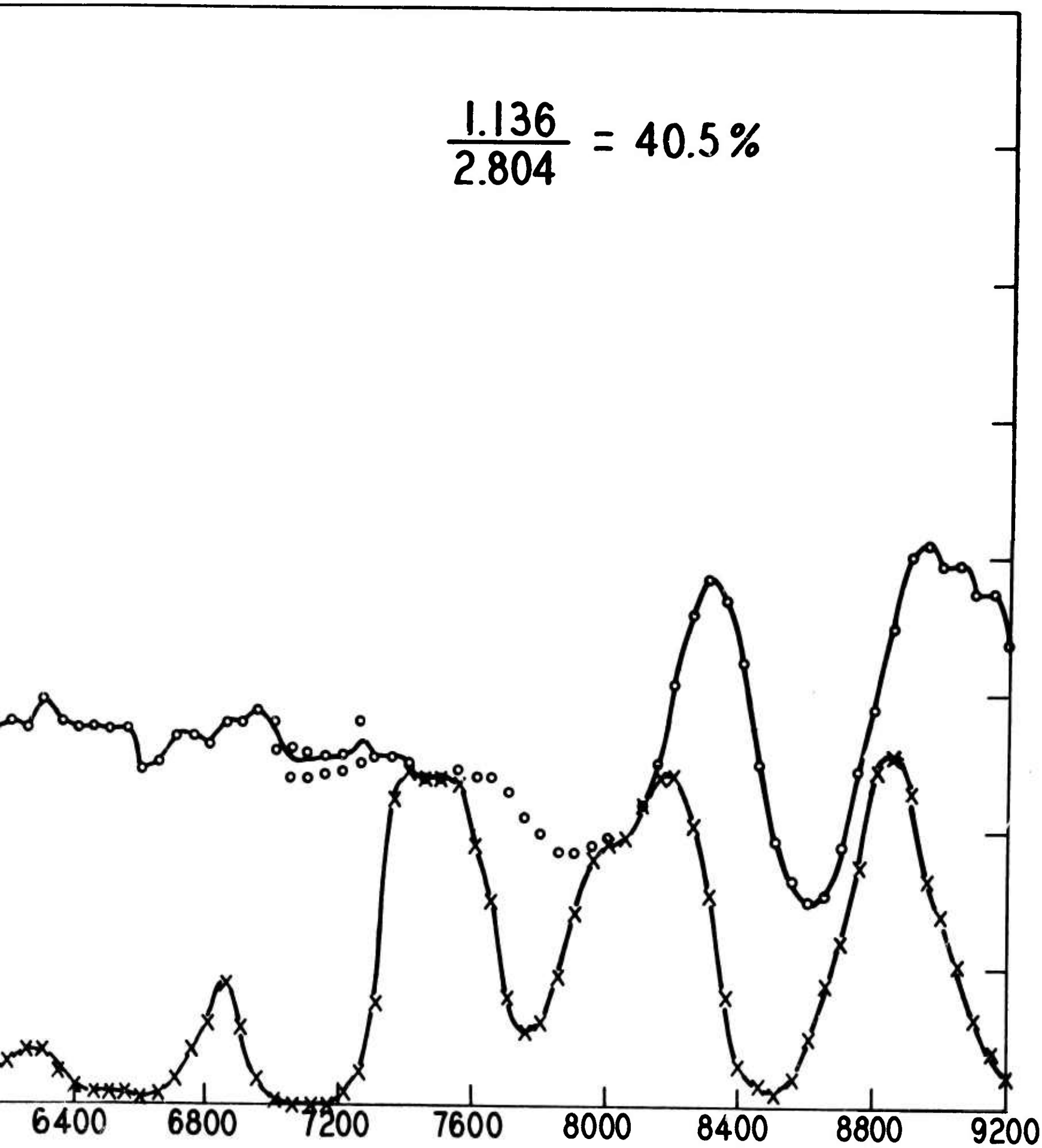

F

FX-95C-4 LAMP SPE

325μf-

5

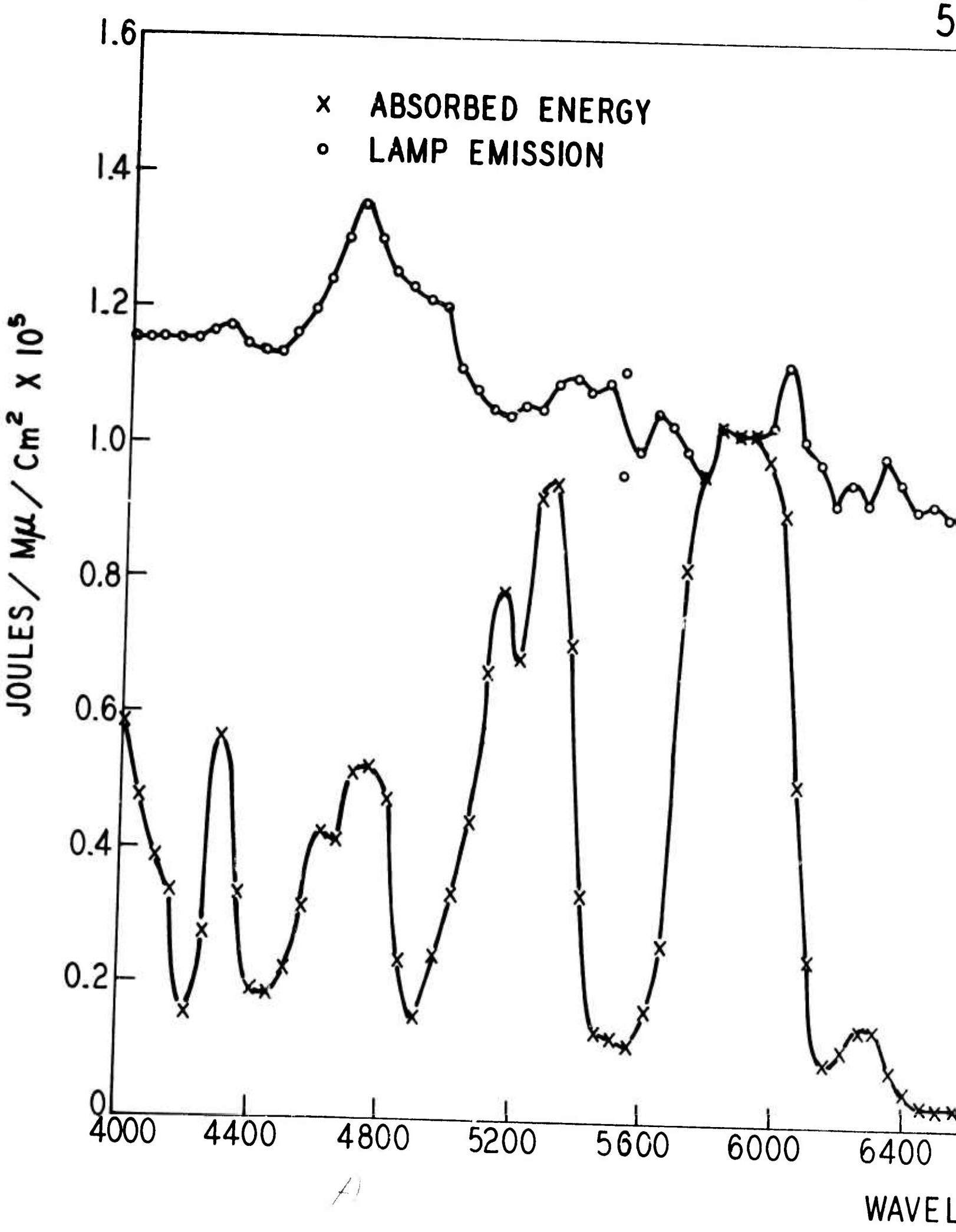

FIGURE 23

P SPECTRAL CHARACTERISTICS
5μf - 100μh LUMPED
5.0 KV

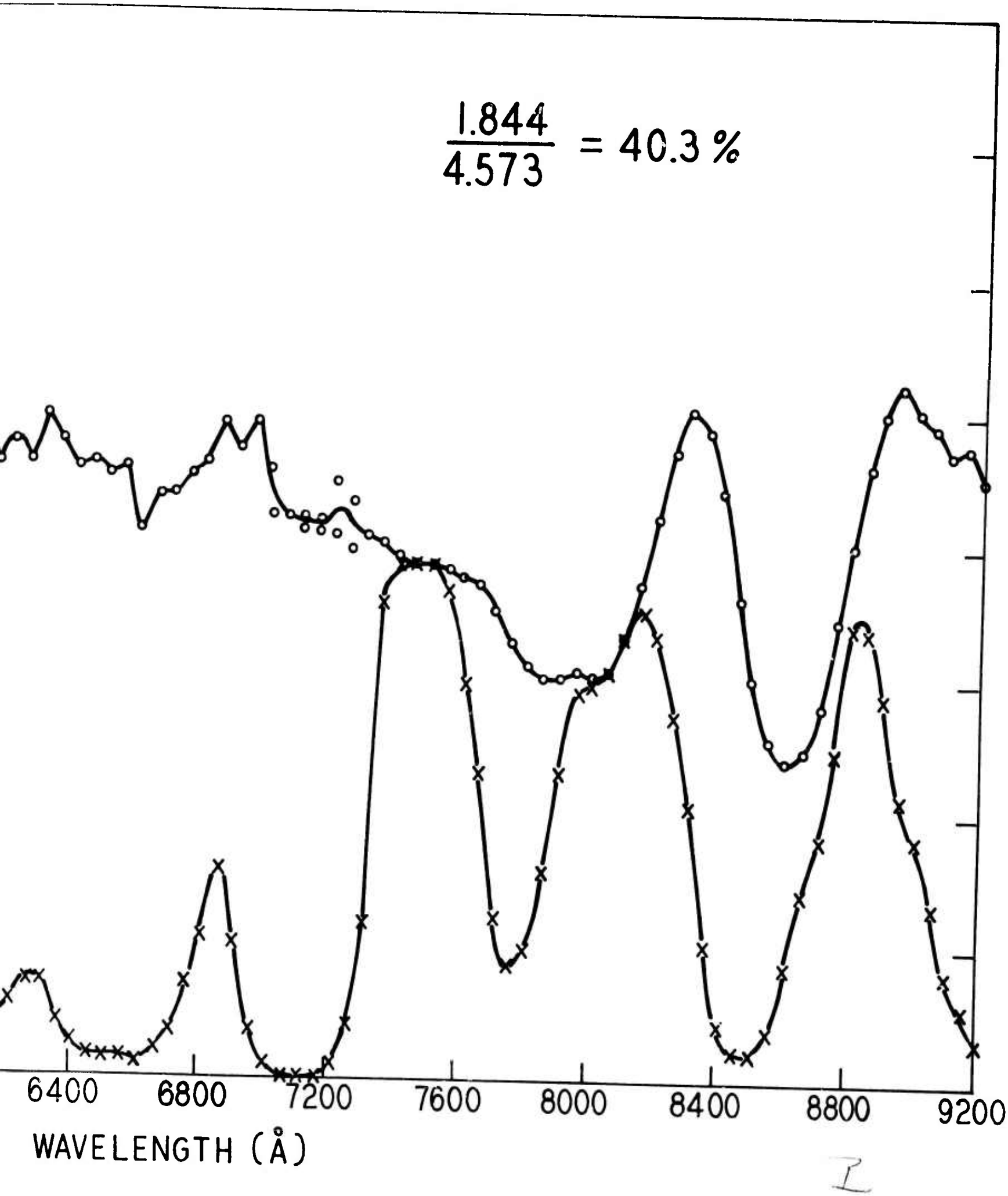

I

FIG

FX-95C-4 LAMP SPEC
325μf-1(
6.(

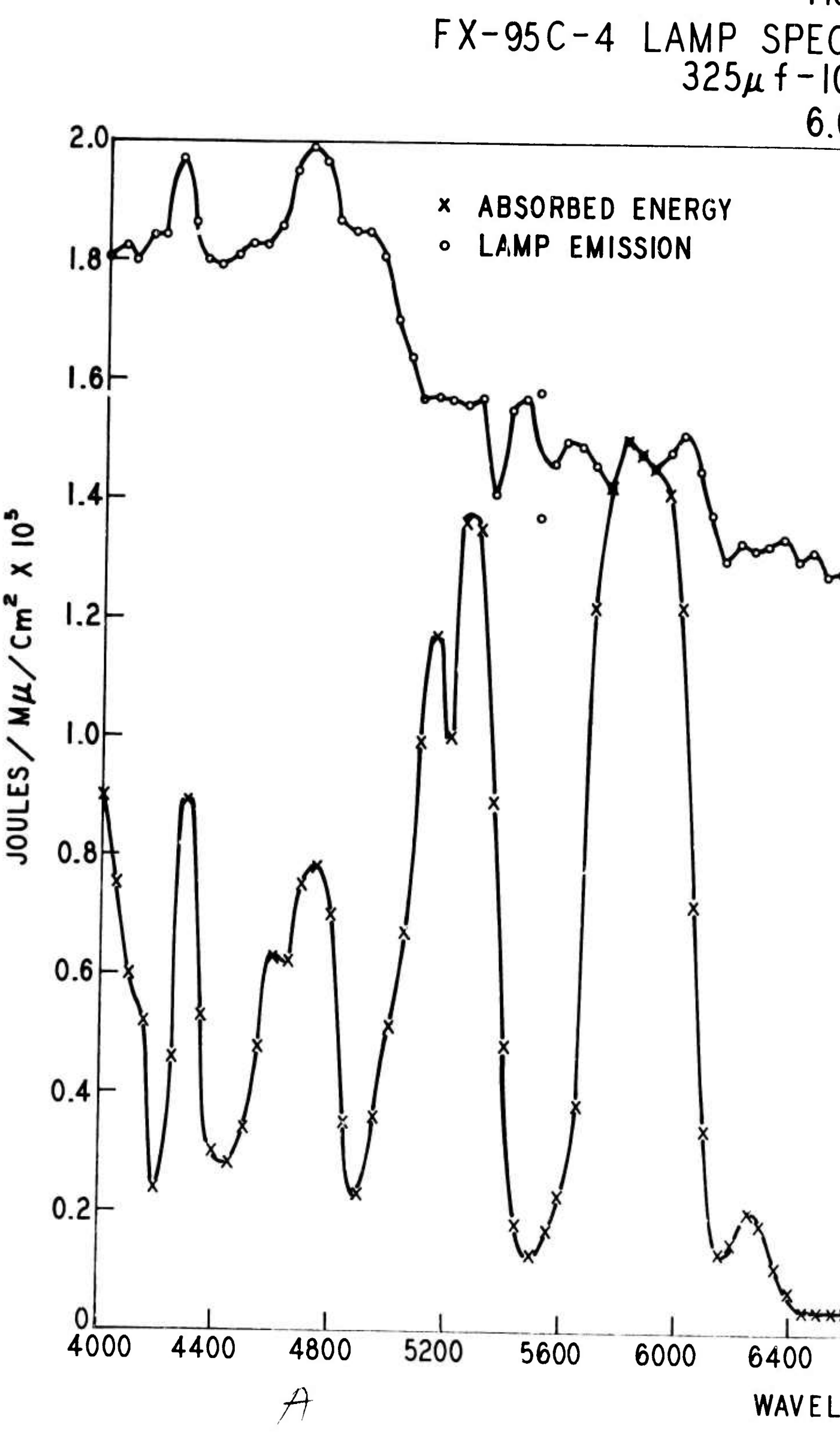

FIGURE 24

SPECTRAL CHARACTERISTICS
μf - 100μh LUMPED
6.0 KV

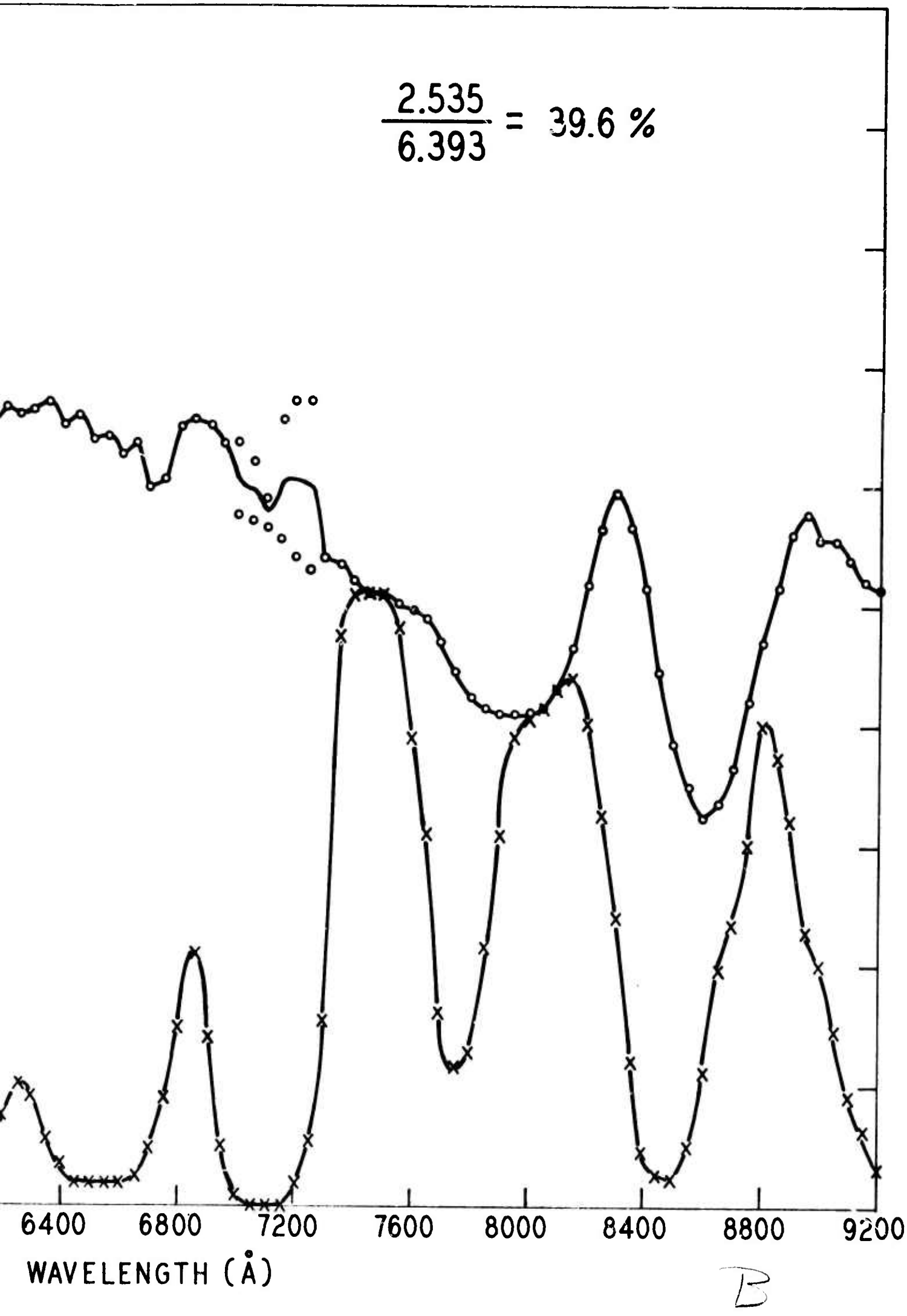

B

3.3 (Continued)

emitted between 4000 Å and 9200 Å is shown in Table 5. When the ratio of the energy absorbed to the energy emitted is considered for the four pump levels, the percent absorption is found to decrease with increased pumping as shown in Table 6. When the K values are adjusted for the lamp spectral shift the values shown in Table 7 result.

The residual variations of K must result from amplified spontaneous emission and/or upper level absorption losses. At present we tend to favor the amplified spontaneous emission loss mechanism, although as yet we can neither separate not measure these two losses. The stored energy loss from these effects is presented in Table 8.

TABLE 5

KV	PERCENT VARIATION OF THE TOTAL LIGHT OUTPUT BETWEEN 4000 Å AND 9200Å
3.0	-18.7%
4.0	- 5.0%
5.0	-
6.0	- 5.5%

TABLE 6

KV	PERCENT OF EMITTED LIGHT ABSORBED BETWEEN 4000 Å AND 9200 Å
3.0	41.0%
4.0	40.5%
5.0	40.3%
6.0	39.6%

TABLE 7

KV	K ADJUSTED FOR LAMP SPECTRAL SHIFT
3.0	0.0063
4.0	0.0065
5.0	0.0055
6.0	0.0051

TABLE 8

KV	STORED ENERGY LOSS FROM RESIDUAL K VARIATIONS
3.0	-
4.0	1.6
5.0	10.6
6.0	19.9

4. DAMAGE THRESHOLD MEASUREMENTS

4.1 Active Damage Tests

Active damage threshold measurements have been obtained for six third amplifier rods selected from three billets A, B, and C. The billets were suspected of containing an unusually high content of platinum due to their respective sparkler contents of 0.46 sparklers/in^3, o.38 sparklers/in^3, and 0.50 sparklers/in^3. The commercial acceptance level for sparklers is 0.08 sparklers/in^3. Four rods were selected from billet A and one each from billets B and C. The damage thresholds for the six samples are presented in Table 9. For the first sample the pulse width was 50 nano-sec and for the last five samples the pulse width was nominally 100 nano-sec. The system full angle beam divergence was for all cases 0.5 milli-radians across the TIR roof edge and 1.5 milli-radians along the TIR roof edge. The system beam profile was not monitored during the test, although subsequent system beam profile measurements do indicate that the peak to average energy density is at least 1.6 for all samples except number six, for which the peak to average is about 1.3 (see Section 2.4). This would result in an average peak energy density damage threshold of 17.8 joules/cm^2 for the six samples evaluated. This test will serve as a reference from which further progress in the melting of laser glass in platinum may be evaluated.

TABLE 9

SAMPLE NUMBER	BILLET	DAMAGE THRESHOLD AVERAGE JOULES/CM^2	DAMAGE THRESHOLD PEAK JOULES/CM^2
1	A	8.0	12.8
2	A	10.8	17.3
3	A	12.0	19.2
4	A	6.8	10.9
5	B	9.8	15.7
6	C	23.9	31.1

4.1 (continued)

One of the damaged amplifier rods was immersed in a cell containing 1.560 immersion oil to examine the inclusions. Three photomicrographs of different defect shapes found in the rod are shown in Figures 25a through 25c. The pictures were taken in normal transmitted light at 30X. The largest defect was photographed at 100X and is shown in Figure 25d. No information on the source of the defects was obtained since only the reflection from the fractured surfaces is seen. The fracture appears to open a lenticular crack, with crushed glass fragments and the fracture source in the interior. This type of fracture is possibly the cause of system component damage which readily appears after internal amplifier damage has developed.

A sample containing inclusions surrounded by acicular crystals as shown in Figure 26 was analyzed by the electron microprobe. The inclusion is about 60 microns by 120 microns and the crystals are about 120 microns long. The sample was polished until the inclusion was observed on the surface. Figure 27 is the electron backscatter image of the inclusion which indicates differences in atomic number. The white area represents the inclusion which is the highest atomic number present. The gray area with fringes is interpreted as inclusion below the section surface and the dark shadows surrounding the inclusion represent the crystals. Figure 28 identifies the inclusion as platinum by the platinum X-ray image. No attempt was made to identify any alloy metal which may be present with the platinum.

PHOTOMICROGRAPHS OF DAMAGE SITES

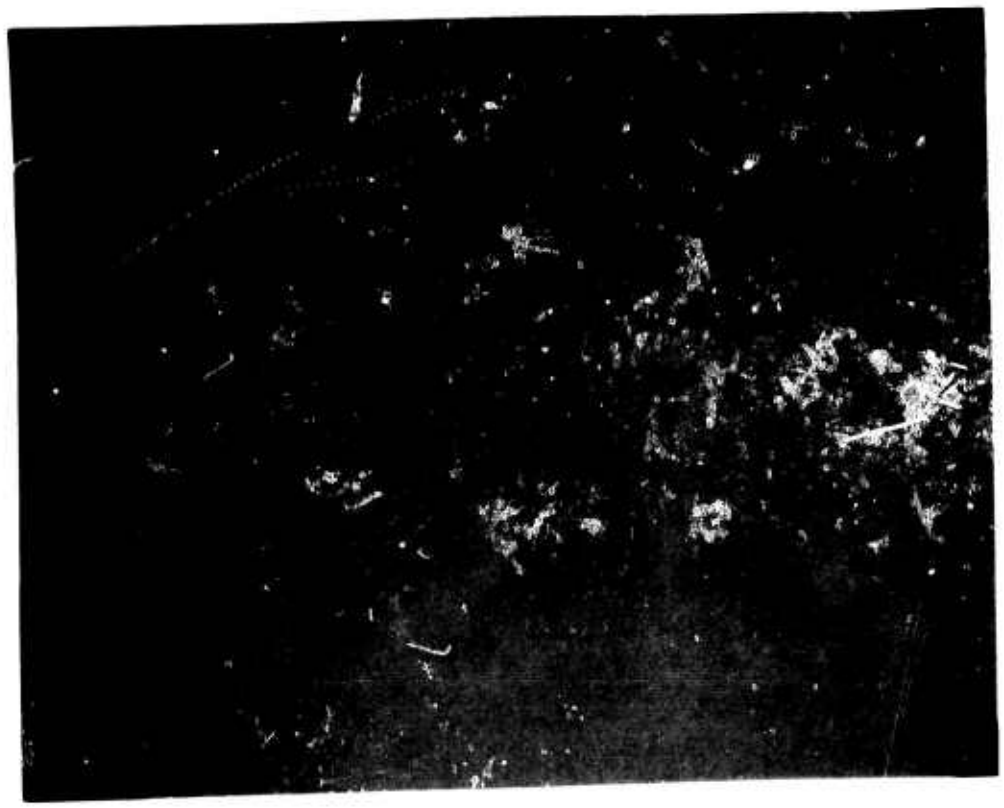

30X

FIGURE 25a

30X

FIGURE 25b

PHOTOMICROGRAPHS OF DAMAGE SITES

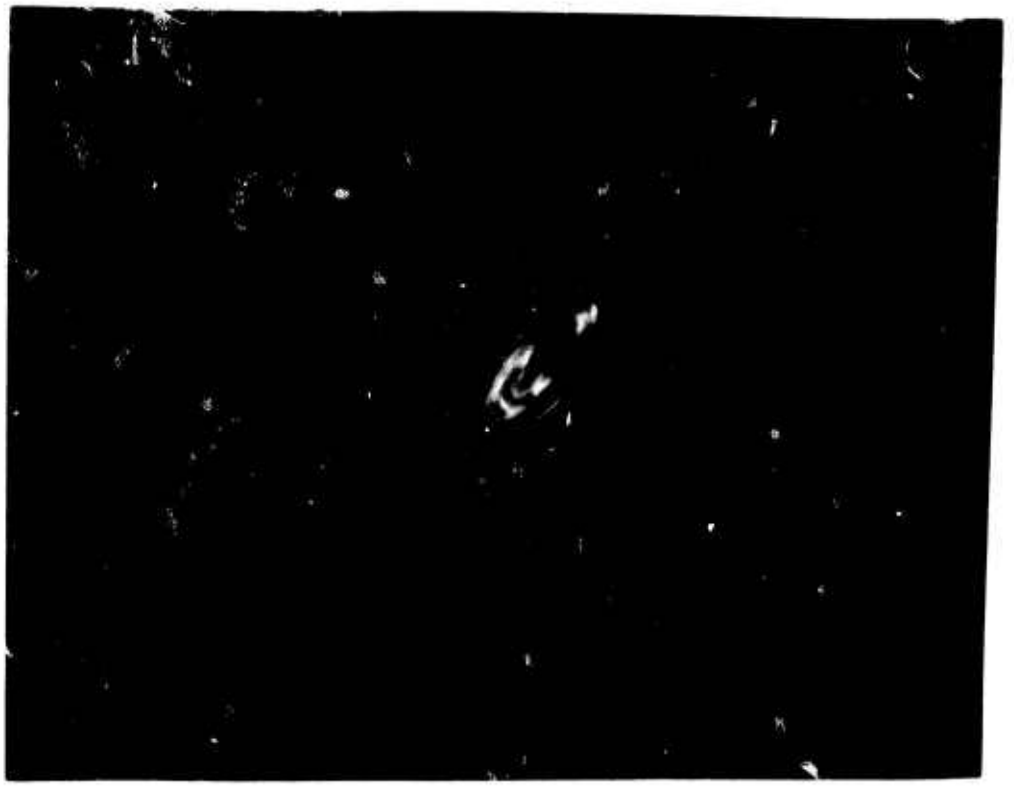

30X

FIGURE 25c

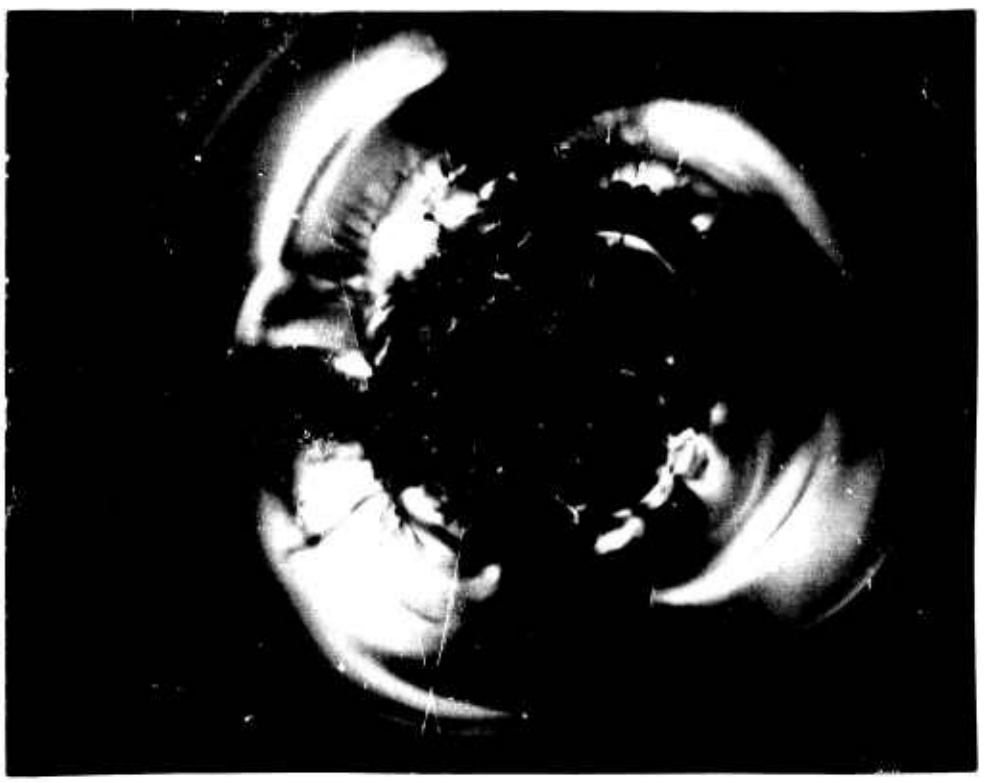

100X

FIGURE 25d

PHOTOMICROGRAPH OF AN INCLUSION PRIOR
TO IRRADIATION

76.5X

FIGURE 26

INCLUSION ELECTRON BACKSCATTER IMAGE

30 μ

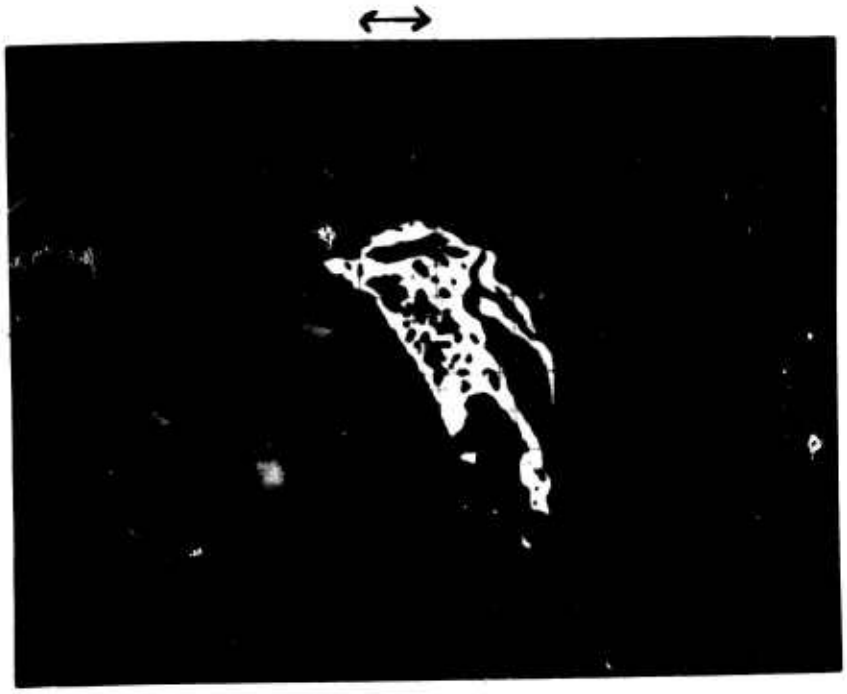

FIGURE 27

INCLUSION PLATINUM X-RAY IMAGE

FIGURE 28

4.2 Passive Damage Tests

A 3/4" cube of laser glass suspected of containing an unusually high platinum content was inspected with a microscope at 44X to determine the location, size and type (crystal or agglomerate) of inclusions present in the sample. The minimum detectable particle size was estimated to be 5 microns. Sixteen inclusions were found prior to irradiation with a size range from 8 by 10 microns to 18 by 93 microns. Twelve of the inclusions were identifiable as crystal. A one cm^2 area of the sample was irradiated with a peak energy density of 8 joules/cm^2 (5 joules/cm^2 average) and the sample was remapped. Approximately fifty new inclusions were found in the sample while only two of the original sixteen had increased in size. The sample was then irradiated with a peak energy density of 21 joules/cm^2 (15 joules/cm^2 average). When again viewed under the microscope approximately six hundred and fifty inclusions were present. To detect the probable cause for such a large number of damage sites a corner of the sample, not previously irradiated, was inspected at 100X. A high density of inclusions (approximately 200/cm^2) with halo diameters 2 microns or smaller were visible; however, their visibility was very sensitive to the lighting. They appeared only with side lighting and were not detectable with direct lighting.

Future samples for passive testing will be cut to a 2mm thickness and mapped at 100X in an attempt to locate these small inclusions prior to irradiation. At present, we are at a loss to identify the type of these sub-micron inclusions.

4.3 Life Tests

Two third amplifier rods have been life tested at a peak energy density of 36 joules/cm^2 (30 joules/cm^2 average). Fifty shots were obtained from the first sample at which time the output end of the rod catastrophically fractured about one inch from the output face. Eighty-five shots were obtained from the second rod before a large hole (4 mm diameter) formed in the output face. The rod end was refinished and after twenty additional shots the output face again damaged in the same location. This type of damage is thought to result from the lenticular inclusions which form within the rod during testing.

For each test the pulse width remained at 50 nano-sec and the beam divergence remained constant at 1.0 milli-radian across the TIR roof edge and 2.0 milli-radians along the TIR roof edge. At the end of each test thirty to forty inclusions were present; however, the system efficiency did not change until the output face damage became severe.

Life testing at 40 joules/cm^2 average intensity was attempted; however, surface damage to system components indicates that this level is unrealistic for life testing at this time.

5. NRL PROGRAM

In addition to the gain and damage measurements discussed in Section 3.1, a complete set of ED-2 rods was evaluated in the NRL CGE VD320 French laser system. They consisted of a 16 mm by 25 cm oscillator rod, a 23 mm by 32 cm first amplifier rod, and a 32 mm by 24.8 cm second amplifier rod. A 3 joule pulse in 30 nano-sec was obtained from the oscillator with two-thirds of the French input. Running the system at 15 joules/cm^2 peak intensity some damage was noted in the second amplifier while no damage appeared in the oscillator or first amplifier.

A more complete and in depth discussion of the NRL program will be presented in their ARPA sponsored contract report.

6. NBS PROGRAM

A 1.5 in. by 1.5 in. by 12 in. sample of platinum melted laser glass has been delivered to NBS. The statistics of the damage threshold within the sample from area to area will be evaluated with their oscillator-amplifier system by focusing through the sample with a long focal length lens.

In an attempt to detect the amount of platinum present in ED-2 laser glass the forward scattering loss coefficient was measured for two samples (one high in platinum content and one low in platinum content). The loss was found to be extremely low and the technique was thereby found to be inadequate for the detection of platinum.

Many additional techniques are being considered by NBS for the detection of platinum prior to irradiation. A more complete discussion of this work will be presented in their ARPA sponsored contract report.